https://doi.org/10.5194/acp-2021-8
Preprint. Discussion started: 29 January 2021

Atmospheric Chemistry and Physics Discussions

The importance of sesquiterpene oxidation products for secondary organic aerosol formation in a spring-time hemi-boreal forest

Luis M. F. Barreira[1,2], Arttu Ylisirniö[1], Iida Pullinen[1], Angela Buchholz[1], Zijun Li[1], Helina Lipp[3], Heikki Junninen[3], Steffen M. Noe[4,5], Alisa Krasnova[4,5], Dmitrii Krasnov[4,5], Kaia Kask[5], Eero Talts[5], Ülo Niinemets[5], Jose Ruiz-Jimenez[6], Siegfried Schobesberger[1]

[1]Department of Applied Physics, University of Eastern Finland, Kuopio, Finland
[2]Atmospheric Composition Research, Finnish Meteorological Institute, Helsinki, Finland
[3]Laboratory of Environmental Physics, Department of Bio and Environmental Physics, University of Tartu, Estonia
[4]Institute of Forestry and Rural Engineering, Estonian University of Life Sciences, Tartu, Estonia
[5]Institute of Agricultural and Environmental Sciences, Estonian University of Life Sciences, Tartu, Estonia
[6]Department of Chemistry and Institute for Atmospheric and Earth System Research, P.O. Box 55, FI-00014 University of Helsinki, Finland

Correspondence to: Luis M. F. Barreira (luis.barreira@fmi.fi)

Abstract. Secondary organic aerosols (SOA) formed from biogenic volatile organic compounds (BVOCs) constitute a significant fraction of atmospheric particulate matter and have been recognized to affect significantly the climate and air quality. Many laboratory and field experiments have studied SOA particle formation and growth in the recent years. Most of them have focused on a few monoterpenes and isoprene. However, atmospheric SOA particulate mass yields and chemical composition result from a much more complex mixture of oxidation products originating from many BVOCs, including terpenes other than isoprene and monoterpenes. Thus, a large uncertainty still remains regarding the contribution of BVOCs to SOA. In particular, organic compounds formed from sesquiterpenes have not been thoroughly investigated, and their contribution to SOA remains poorly characterized. In this study, a Filter Inlet for Gases and Aerosols (FIGAERO) combined with a high-resolution time-of-flight chemical ionization mass spectrometer (CIMS), with iodide ionization, was used for the simultaneous measurement of gas and particle phase atmospheric SOA. The aim of the study was to evaluate the relative contribution of sesquiterpene oxidation products to SOA in a spring-time hemi-boreal forest environment. Our results revealed that monoterpene and sesquiterpene oxidation products were the main contributors to SOA particles. The chemical composition of SOA particles was compared for times when either monoterpene or sesquiterpene oxidation products were dominant and possible key oxidation products for SOA particle formation were identified. Surprisingly, sesquiterpene oxidation products were the predominant fraction in the particle phase at some periods, while their gas phase concentrations remained much lower than those of monoterpene products. This can be explained by quick and effective partitioning of sesquiterpene products into the particle phase or their efficient removal by dry deposition. The SOA particle volatility determined from measured thermograms increased when the concentration of sesquiterpene oxidation products in SOA particles was higher than that of monoterpenes. Overall, this study demonstrates the important role of sesquiterpenes in atmospheric chemistry and suggests that the contribution of their products to SOA particles is being underestimated in comparison to the most studied terpenes.

https://doi.org/10.5194/acp-2021-8
Preprint. Discussion started: 29 January 2021

Atmospheric Chemistry and Physics Discussions

1 Introduction

Volatile organic compounds (VOCs) are ubiquitous constituents of Earth´s atmosphere that are emitted from both biogenic and anthropogenic sources (e.g. Kansal, 2009). Anthropogenic VOCs (AVOCs) may predominate in urban areas, but the source strength of biogenic VOCs (BVOCs) exceeds that of AVOCs by an order of magnitude, implying that BVOCs dominate on the global scale (e.g. Guenther et al., 1995; Kansal, 2009) and often even in urban environments (e.g. Barreira et al., 2020). BVOCs are mostly emitted by vegetation in relation to temperature and/or light, but recently plant damages (e.g. due to herbivore attack), and the resulting wound emissions and *de novo* induced emissions, have been also recognized as important factors impacting emissions of BVOCs (e.g. Grote et al., 2013; Kari et al., 2019; Laothawornkitkul et al., 2009; Niinemets, 2018; Niinemets et al., 2013; Peñuelas and Staudt, 2010). BVOCs are vital in nature since they participate in several processes, such as the defense of plants against predators or communication between species (e.g. Peñuelas and Staudt, 2010). BVOCs also play an important role in atmospheric physics and chemistry. They react with atmospheric oxidants, which result in the formation of secondary products (e.g. Kavouras et al., 1999). Ultimately, these oxidation products can contribute to secondary organic aerosol (SOA) particle formation and growth (e.g. Riipinen et al., 2012). SOA influences the Earth's radiative balance by scattering and absorbing solar radiation and by acting as cloud condensation nuclei (e.g. Ezhova et al., 2018; Hallquist et al., 2009). Aerosols in the atmosphere also have adverse effects on public health, since they cause or enhance respiratory, cardiovascular, infectious and allergic diseases (Pöschl, 2005).

The most abundantly emitted biogenic species are terpenes, a very heterogeneous compound class. Terpenes have high structural diversity, such as distinct double bond amounts and positions. Due to their structural diversity, terpenes display a wide range of reactivities against atmospheric oxidants, and thus their lifetimes vary considerably between different species (Atkinson and Arey, 2003). For that reason, the distribution of terpene-derived oxidation products depends on their specific precursors and on the atmospheric abundance of a variety of reaction partners (O_3, HO_x, NO_3, and NO_x) (e.g. Atkinson and Arey, 2003; Jokinen et al., 2015). Isoprene and monoterpenes are the most studied SOA precursor terpenes in boreal environments, but the interest in the role of sesquiterpenes has recently grown with the increasing availability of measurement techniques suitable for detection and quantification of sesquiterpenes and their oxidation products. For example, a recent study has found that sesquiterpenes have a larger effect on ozone (O_3) chemistry and higher production rates of condensable organic vapors when compared to monoterpenes (Hellén et al., 2018). As sesquiterpene oxidation products are generally expected to be less volatile than monoterpene oxidation products, they may play a stronger role on the local SOA formation and particle growth (Hellén et al., 2018). However, in comparison to monoterpenes, the contribution of sesquiterpenes to SOA has been often overlooked due to challenges in measuring these highly reactive atmospheric constituents.

In this study, comprehensive field measurements of atmospheric gas and particle phase composition were performed in the spring of 2018 at the SMEAR (Station for Measuring Ecosystem-Atmosphere Relations) Estonia in Järvselja, Estonia. The study was part of the Järvselja 2018 Campaign, which aimed to study both new particle formation and SOA composition in a hemi-boreal forest. As our measurements were performed during springtime, they covered a period of significant changes in

https://doi.org/10.5194/acp-2021-8
Preprint. Discussion started: 29 January 2021


Atmospheric Chemistry and Physics Discussions

biosphere activity. The aerosol composition was characterized by using both on-line and off-line methods. The on-line measurements were performed by employing a Filter Inlet for Gases and Aerosols combined with high-resolution time-of-flight chemical ionization mass spectrometry (FIGAERO-CIMS). Aerosol particle samples were also collected on filters for off-line analysis by liquid chromatography combined with electrospray ionization quadrupole time-of-flight mass spectrometry (LC-QToF-MS) and by gas chromatography combined with chemical ionization quadrupole time-of-flight mass spectrometry (GC-QToF-MS). The main aim of this study was to investigate the importance of sesquiterpenes to SOA composition.

2 Material and methods

2.1 Measurement site

Comprehensive on-line measurements were performed in spring 2018 from 23rd of April to 29th of May at SMEAR Estonia. This station is located in the Järvselja forest (58.2776°N, 27.3083°E, 36 m a.s.l.), which consists of a hemi-boreal forest stand comprising mostly Scots pine (*Pinus sylvestris* L.), Norway spruce (*Picea abies* (L.) Karst.), silver birch (*Betula pendula* Roth.), and downy birch (*Betula pubescens* Ehrh.). The dominant tree species are Scots pine, followed by Norway spruce and birch species. The mean canopy height was 20 m, but within about 300 m around the station the oldest stands could reach up to 30 m. The main cities nearest to the site are Tartu (about 100 000 inhabitants, 36 km west-northwest) and Pskov (about 205 000 inhabitants, 79 km southeast across Lake Peipus). The mean annual temperature in the area varies between 4 and 6 °C, with temperature ranging between -5 and 28 °C during the campaign period. The annual precipitation is 500–750 mm, with about 40–80 mm as snow, and the growing season length is about 170–180 days. The location qualifies as rural background monitoring site. A detailed description of the site can be found in Noe et al. (2015). The on-line instruments used in this study were installed inside a measurement container located approximately 10 m from the nearest trees.

2.2 Measurement methods

2.2.1 FIGAERO-CIMS

Measurements of inorganic and organic compounds in both gas and particle phase were performed by FIGAERO-CIMS using iodide ionization (HR-ToF-CIMS, Aerodyne Research Inc.). The used FIGAERO unit had been custom-built in early 2018 and differs slightly from other designs generally used (Ylisirniö et al., 2020a), but the main operation principles are the same as in Lopez-Hilfiker et al. (2014). The overall sampling setup used in this study is presented in Fig. S1. The FIGAERO-CIMS measurement cycle involved 45 minutes of gas phase measurements and simultaneous particle collection, followed by 45 minutes of aerosol particle desorption and measurements. The gas phase sampling line was operated with 15 L min^{-1} flow. This high flow limits vapor-wall interactions, such as wall-losses for low-volatility compounds. The FIGAERO-CIMS instrument subsampled 2.1 L min^{-1} from close to its inlet. Teflon tubing (~2 meters of 1.27 cm outer diameter tubing followed

https://doi.org/10.5194/acp-2021-8
Preprint. Discussion started: 29 January 2021


Atmospheric Chemistry and Physics Discussions

by 3 cm of 0.635 cm outer diameter tubing closer to the instrument inlet) was used for the gas phase inlet. For aerosol particle collection, a cyclone was used to selectively collect particles with an aerodynamic diameter below 1 µm (PM_1). The total flow through the cyclone was 11 L min^{-1}, which was then split into 5.5 L min^{-1} for the FIGAERO aerosol particle collection and 5.5 L min^{-1} for off-line filter collection. Copper tubing (2 meters with an outer diameter of 10 mm) was used for the sampling of aerosol particles. The desorption step consisted of a 30 minutes linear temperature increase from room temperature to 200 °C (approx. 5.8 °C min^{-1}). The temperature was held at 200 °C for 15 additional minutes to ensure that all detectable organic material was removed from the filter. Gas and particle phase blanks were also measured. The gas phase blanks were performed by introducing dry ultra-high-purity N_2 a few cm away from the critical orifice to displace the incoming ambient air. The N_2 flow was closed during sampling and only opened for blanks. These blanks were conducted for 10 seconds following a period of 50 seconds of gas phase measurements. Particle phase blanks were obtained by adding a HEPA filter in the sampling line to remove all particles before using the same collection and measurement method as for the samples. One particle phase blank was collected after three particle samples. A detailed description of FIGAERO-CIMS data processing is presented in the supplemental material (Sect. S2).

2.2.2 Off-line filter analysis

For comparison purposes, PM_1 was also collected on PTFE filters for off-line analysis. The collection time was about 4 days at a sampling flow of 5.5 L min^{-1}. The filters were stored in a freezer at −18 °C. For sample preparation, the filters were extracted in 10 mL of acetonitrile and sonicated for 30 minutes as in Duporté et al. (2016). Then, a gentle stream of nitrogen was used to reduce the extracts to 250 µL.

Half of the sample was kept in acetonitrile for LC-QToF-MS analysis. The analytical method is described in Puurunen et al. (2016) and in the supplemental material (see Sect. S3). Briefly, the LC-QToF-MS (Agilent Technologies, Waldbronn, Karlsruhe, Germany) consisted of a 1290 LC system, a Jetstream electrospray ionization (ESI) source and a 6540 UHD accurate-mass quadrupole-time-of-flight (QToF) mass spectrometer. All samples were analyzed using reversed phase (RP) chromatography. The data was acquired in both ionization polarities; i.e., ESI positive (ESI^+) and ESI negative (ESI^-). The resolution was between 12000 and 25000 (from 118 m/z to 622 m/z).

The other half of the sample was reduced to 10 µL and reconstituted in 100 µL of dichloromethane for analysis with a 7200 accurate-mass GC-QToF-MS instrument (Agilent Technologies, Santa Clara, CA), operating in negative chemical ionization mode, to measure the volatile and/or semi-volatile fraction of the aerosol particles. The resolution was between 11000 and 21000 (from 185 m/z to 517 m/z). A detailed description of the operational parameters used for GC-QToF-MS can be found in the supplemental material (Sect. S3).

For both LC-QToF-MS and GC-QToF-MS analysis, the measured signal was normalized by the total volume of ambient air collected on the filter. For filter blanks, clean filters were extracted and analyzed with the same methods described above for the filters used in PM_1 sample collection.

https://doi.org/10.5194/acp-2021-8
Preprint. Discussion started: 29 January 2021


Atmospheric Chemistry and Physics Discussions

130 **2.2.3 Auxiliary measurements**

To allow BVOC species distinction, ambient air was sampled into multibed stainless steel cartridges (10.5 cm length, 3 mm inner diameter, Supelco, Bellefonte, PA, USA), which were filled with Carbotrap C 20/40 mesh (0.2 g), Carbopack C 40/60 mesh (0.1 g) and Carbotrap X 20/40 mesh (0.1 g) adsorbents (Supelco) (Kännaste et al., 2014). A volume of 6 L was sampled for 30 minutes intervals once or twice a day using flow-controlled pumps operating at 200 mL min^{-1} (1003-SKC, SKC Inc.,
135 Houston, TX, USA). After sampling, the cartridges were kept in a freezer and transported to the laboratory for GC-MS analysis at least twice a week. Adsorbent cartridges were analyzed with a combined Shimadzu TD20 automated cartridge desorber system linked to a Shimadzu 2010 Plus GC-MS instrument. A more detailed description of the analytical method can be found in Noe et al. (2012).

A proton-transfer-reaction time-of-flight mass spectrometer (PTR-ToF-MS) was also used to monitor the VOC concentrations.
140 The PTR-ToF-MS data was pre-processed (using 10 minutes averaging) with tofTools software (Junninen et al., 2010) for peak shape, mass calibration, UMR stick integration and resolution function. In this software, a quadratic function with 5 masses (corresponding to NH_3H^+, $H_2[^{18}O]H^+$, $O[^{18}O]^+$, $C_3H_6OH^+$, $C_7H_8H^+$ and $C_{10}H_{16}H^+$) was used for mass calibration. Altogether, 238 peaks were identified.

Additional PM_1 size distribution measurements were performed at the measurement site using a scanning mobility particle
145 sizer (SMPS, TSI Inc. model 3082 + 3776). For comparison purposes, the particle number concentration (PNC) measured by SMPS was converted into particle mass concentration (PMC), assuming a particle density of 1.3 g cm^{-3}. The upper size limit of the SMPS was 800 nm.

Meteorological data (temperature and relative humidity) and other relevant trace gas concentrations (e.g. NO_x, O_3) were continuously measured at the sampling site. Mixing height data was obtained from the NOAA website
150 (ftp://arlftp.arlhq.noaa.gov/pub/archives/gdas1, last access: 13 October 2020). The sunrise and sunset times were obtained from the timeandate.com website (https://www.timeanddate.com/sun/estonia/tartu, last access: 07 December 2020).

2.3 FIGAERO-CIMS calibration

The FIGAERO-CIMS response function was determined by measuring known amounts of acetic acid (gas phase mode) and glutaric acid aerosol (particle phase mode). The limit of quantification (LOQ) was derived as 10 times the average values of
155 15 randomly chosen ions from the mass range of 800 – 1000 Th. More details can be found in the supplement material (Sect. S4).

The concentration of analytes was determined using the obtained calibration coefficients, with the assumption that all analytes have the same instrumental response. The main reason for this approach is the multitude of analytes that are measured in ambient air and the difficulty in finding authentic standards for most of those analytes. CIMS sensitivity depends on several
160 factors, including the molecular functionality, instrument parameters (e.g. inlet temperature and pressure), transmission efficiency, declustering strength, and water vapor pressure (Lee et al., 2014). In particular, for iodide-adduct CIMS, the

https://doi.org/10.5194/acp-2021-8
Preprint. Discussion started: 29 January 2021


Atmospheric Chemistry and Physics Discussions

instrument response depends on the analyte polarity (sensitivity increases with the addition of a polar group), hydrogen bonding capacity, molecular geometry and molecular size (Iyer et al., 2016; Lopez-Hilfiker et al., 2016). The ensuing considerable variations in sensitivity for compounds detectable in ambient samples and the susceptibility of some analytes to thermal decomposition are further reasons why we present results as semi-quantitative, even though we often report them as concentrations. Additional limitations associated to the analytical method used in this study are discussed in the supplemental material (Sect. S5).

The volatility of organic aerosol components (expressed as saturation mass concentrations at 25 °C, C^*) was obtained both based on the ion thermograms and by using a parametrization based on the elemental composition determined by soft-ionization high-resolution mass spectrometry techniques (Li et al., 2016). The thermogram-based volatility was determined as described by Ylisirniö et al. (2020b). The T_{max} values of each detected ion were converted to the corresponding P_{sat} using Eq. (1):

$$P_{sat} = exp^{a}\, exp^{b\, Tmax} \quad , \tag{1}$$

where a and b are fitted parameters from calibration measurements with atomized compounds of known volatility (Ylisirniö et al., 2020b). The used calibration values for the fit are shown in Sect. S3. The calibration parameters were a = -3.92 and b = -0.13 (K^{-1}). P_{sat} values were converted to C^* (μg m^{-3}) by using the following Eq. (2):

$$C^* = \frac{P_{sat}\, M_W}{R\, T_{amb}} 10^6 \quad , \tag{2}$$

where M_w is the molar mass without iodide, R is the gas constant (8.3144 Pa m^3 K^{-1} mol^{-1}), and T_{amb} (K) is the ambient temperature (set to 298 K).

On the other hand, for the parameterization method, the volatility was calculated for each detected compound by the Eq. (3):

$$log_{10} C_O = (n_C^O - n_C) b_C - n_O\, b_O - 2\, \frac{n_C\, n_O}{n_C + n_O} b_{CO} - n_N\, b_N - n_s\, b_s \quad , \tag{3}$$

where n^0_C is the reference carbon number (25); n_C, n_O, n_N, and n_S denote the numbers of carbon, oxygen, nitrogen, and sulfur atoms, respectively; b_C, b_O, b_N, and b_S denote the contribution of each atom to $log_{10}C_0$, respectively; and b_{CO} accounts for the carbon–oxygen nonideality (Donahue et al., 2011; Li et al., 2016). The equation is based on a previous parameterization developed by Donahue et al. (2011) for CHO compounds, but optimized to be applicable for N- and S-containing compounds.

2.4 Grouping of chemical formulas to investigate terpene oxidation products

Since the purpose of this study was to investigate the role of different terpene oxidation products on SOA particle formation, the measured chemical formulas were grouped by their elemental composition according to the presumed precursor terpene classes (Table 1). Specifically, we presumed that $C_{7\text{-}10}H_{<=(1.8xC)}O_z$ compounds originated from oxidation of monoterpenes (o-MT group) and $C_{13\text{-}15}H_{<=(1.75xC)}O_z$ compounds from oxidation of sesquiterpenes (o-SQT group). For comparison purposes, other chemical formulas were also grouped, including: $C_{>=17}H_{<=(1.8xC)}O_z$, which include many conceivable dimers of monoterpene oxidation products but can also include diterpene oxidation products (Dimers group), and $C_{4\text{-}5}H_{<=(2.4xC)}O_z$ (o-$C_{4\text{-}5}$ group). These o-$C_{4\text{-}5}$ compounds would presumably include many isoprene oxidation products but can as well comprise short-chained

https://doi.org/10.5194/acp-2021-8
Preprint. Discussion started: 29 January 2021


Atmospheric Chemistry and Physics Discussions

products from C-C bond scission reactions of mono- and sesquiterpenes, or, in the particle phase, products formed by thermal decomposition of larger, lower-volatility compounds during the desorption phase of the FIGAERO-CIMS analysis.

The classification based on the number of H atoms (#H) was performed by considering the oxidative reactions of terpenes. For example, the oxidation of α-pinene, the prevailing emitted terpene at the sampling site (Fig. S2), has been found to generate oxidation products of up to #H=18 (through a chain of reactions initialized by the OH/O_3 attachment to the double bond) (e.g. Li et al., 2019a). The same classification criterion was applied for other groups. However, the tentative identification of chemical formulas revealed the possible presence of compounds with unusually high H:C ratio (higher than 18:10). Due to the limited CIMS resolution, their presence could not be definitely confirmed (Sect. S5), and thus these compounds were grouped separately as $C_{9\text{-}11}H_{(>1.8xC)}O_z$ (o-highH1 group) and $C_{>=12}H_{(>1.8xC)}O_z$ (o-highH2 group). Some of the major contributors to the o-highH1 group, such as $C_{10}H_{20}O_6$, $C_{10}H_{20}O_7$ and $C_{10}H_{22}O_7$, have been previously connected to wet and acidic isoprene-derived SOA (Riva et al., 2016) and/or assigned as monoterpene SOA (Zhang et al., 2018). However, the chemical pathway to those highly to fully saturated compounds has remained unknown.

Organonitrates were classified as $C_xH_yO_zN_{>0}$ (ON group) and compounds that did not fit any of the afore-mentioned groups, such as inorganics (e.g. HNO_3, H_2SO_4) and small thermal-decomposition products (but excluding reagent ions), were classified as "others".

3 Results and discussion

In this study, gas and particle phase compositions and concentrations were measured to assess the contribution of sesquiterpene oxidation products to SOA. A campaign overview is firstly presented and an in-depth investigation of periods with high aerosol particle mass loadings is subsequently described.

3.1 Campaign overview

3.1.1 Atmospheric particle and gas phase concentrations

The summed mass concentrations of analytes in particle phase, measured by FIGAERO-CIMS, were compared with PM_1 determined by SMPS. As seen in Fig. 1, the summed particle phase analyte concentrations tracked the changes in SMPS-derived PM_1, broadly validating our analytical method and suggesting that PM_1 was dominated by organic aerosol (OA) throughout the campaign. However, a significant difference in absolute concentrations was observed between the results obtained by the mentioned techniques, with PM_1 measured by SMPS being about 4 times higher than the one measured by FIGAERO-CIMS. The differences may be attributed to the increasing selectivity of iodide CIMS with analyte polarity, the fact that detection with FIGAERO-CIMS is limited to analytes that can be thermally desorbed from the filter, and uncertainties in the calibration procedure (see Sect. S4 in supplement material).

The highest PM_1 occurred between 13th and 18th of May (Fig. 1). The observed increase in particulate mass during that time period was consistent with an overall increase in temperature and photosynthetically active radiation (PAR), the chief drivers

https://doi.org/10.5194/acp-2021-8
Preprint. Discussion started: 29 January 2021


Atmospheric Chemistry and Physics Discussions

of BVOC emissions. A comparison between the sum of gas and particle phase concentrations of larger oxygenated organics ($C_{>3}H_yO_z$) and organonitrates ($C_{>3}H_yO_zN_{>0}$), measured by FIGAERO-CIMS and presumably originated mostly from terpenes oxidation, and atmospheric parameters associated with BVOC emissions and/or SOA concentration (temperature, RH, precipitation, NO_x and O_3) is shown in Fig. 2. Particle phase oxidation products were generally higher during the night, with concentrations starting to increase in the late evening and reaching the maximum during early morning (Fig. 2). On the other hand, gas phase oxidation products peaked during daytime (Fig. 2). The high PM_1 values during night-time are likely explained by the decrease in mixing height and temperature during that period of the day as commonly observed (e.g. Barreira et al., 2020). Although the production of oxidation products occurred predominantly during daytime, the decrease in mixing height during night causes a near-surface accumulation of VOCs, oxidants, oxidation products and aerosol particles, which in combination with the decrease in temperature enhances the partitioning of oxidized compounds and thus favours the formation of SOA particles (e.g. Hao et al., 2018).

Areas upwind of the sampling site might have contributed to the observed SOA composition and concentration. However, the chemical composition measured by FIGAERO-CIMS appears to support a significant influence from locally produced BVOC oxidation products since a decrease in concentration-weighted O:C was generally observed in particle phase (Fig. S3) during night. This decrease suggests the prevalence of "freshly" oxidized products (i.e. with relatively low oxygen content) in aerosol particle composition during that period of the day. However, the higher presence of low oxygenated products in the particle phase could be also caused by more volatile compounds partitioning into the particles due to cooler temperatures observed during night-time.

3.1.2 Chemical characterization of gas and particle phase atmospheric constituents

During this study, a total of 1375 chemical formulas were tentatively identified in gas phase and 1380 in particle phase measurements by FIGAERO-CIMS (above LOQ, Sect. 2.3). Among those, CHO compounds clearly dominated, constituting 68 % of measured gas phase and 78 % of particle phase concentrations on a campaign-wide average (Fig. S4). The second largest group of aerosol constituents were CHON molecules, with percentages of 9 % and 18 % in the gas and particle phase, respectively, while CHOS and CHONS contributed less than 4 % to total measured concentrations for both gas and particle phase. Other compounds, excluding reagent ions, constituted 22 % of gas phase (mostly HNO_3) and 1 % of particle phase concentrations. The predominance of CHO compounds was expected due to the specificity of iodide chemical ionization for oxygen-containing functional groups, especially those containing –O–H moieties (e.g. Lee et al., 2014).

The time series of compound groups (defined in Sect. 2.4), obtained for particle and gas phase measurements, are shown in Fig. 3. The mean, median and maximum concentrations of the defined groups are presented in Table 1. Monoterpene and sesquiterpene oxidation products were the particle phase constituents with highest concentrations during the full campaign period (Fig. 3). The o-MT reached a maximum particle phase concentration of 3.1 µg m^{-3}, while o-SQT particle phase concentrations were up to 1.6 µg m^{-3} (Table 1, Fig. 3). Interestingly, the highly hydrogenated groups also reached high concentrations in the particle phase, with concentrations of up to 1.6 µg m^{-3} and 0.6 µg m^{-3} for o-highH1 and o-highH2,

https://doi.org/10.5194/acp-2021-8
Preprint. Discussion started: 29 January 2021


Atmospheric Chemistry and Physics Discussions

respectively. Organonitrates reached concentrations of up to 1.0 µg m^{-3}. The smaller contribution of organonitrates, when compared to the sum of CHO aerosol particle constituents, is expected due to the low anthropogenic influence (e.g. from traffic) at the measurement site as confirmed by the relatively low NO_x levels (Fig. 2 for NO_x). The maximum particulate concentration of o-C_{4-5} was 0.5 µg m^{-3}, while the particulate concentration of Dimers was up to 0.2 µg m^{-3}. The low Dimers concentration in particle phase indicates that the contribution of diterpenes/monoterpene dimer products to atmospheric particulate mass was small or that those products were particularly susceptible to thermal decomposition or fragmentation in the measurement process. However, these high molecular weighted constituents might still have played an important role in new particle formation due to their expected extremely low (or "ultra-low") volatility and consequent potential to form aerosol nuclei (Lehtipalo et al., 2018; Schervish and Donahue, 2020). Other measured analytes had a contribution to aerosol particulate mass of up to 1.2 µg m^{-3}.

For the gas phase, o-C_{4-5} were the dominant compounds with concentrations of up to 17.0 µg m^{-3} (3.6 ppbv), followed by ON with up to 16.1 µg m^{-3} (2.3 ppbv) and o-MT that reached 6.1 µg m^{-3} (0.8 ppbv). Although ON reached high concentrations in the gas phase, the higher concentrations occurred mostly during traffic pollution events since ON exhibited the same trends as NO_X during those event periods (Fig. 2). All other constituent groups were present in gas phase concentrations below or equal to 0.4 µg m^{-3} (0.04 ppbv). An exception was observed for o-highH1, which had few concentration spikes with a maximum of 6.1 µg m^{-3} (0.6 ppbv). However, these spikes occurred after high concentrations measured in particle phase mode, and a carry-over from previous aerosol measurements cannot be excluded since the volatility of these compounds is probably very low. As they only occur in brief spikes, they will not be captured by the regular blank measurements and cannot be accounted for.

The particle phase o-SQT concentrations were higher than in the gas phase. This result seems to indicate that, generally, sesquiterpene oxidation products partition very quickly into the particle phase, which is corroborated by the theoretical equilibrium constants of these relatively large compounds that indicate essentially irreversible condensation (e.g. Joensuu et al., 2016). Vice versa, the o-C_{4-5} group of analytes was much lower in the particle phase than in the gas phase. These smaller compounds are expected to have higher volatility than monoterpene and sesquiterpene oxidation products, which makes the partitioning into the particle phase more difficult (Donahue et al., 2012). An exceptional increase of $C_6H_{10}O_5$ in the particle phase was observed for some short (<day) episodes, in particular in the beginning of the campaign, with a concentration of up to 0.5 µg m^{-3}, contributing significantly to OA. This molecular formula is likely associated to levoglucosan, which is a well-known wood burning tracer (e.g. Helin et al., 2018). Considering the high atmospheric stability of levoglucosan (e.g. Fraser and Lakshmanan, 2000) and since increased $C_6H_{10}O_5$ concentrations were not observed in the gas phase, it is likely that a long-range transport episode of particulate matter was the cause of high measured concentrations of this constituent. The biomass burning aerosol particles were likely originated in Eastern Europe since the dominant wind direction was from south-east at the time of the episode (Fig, 3).

https://doi.org/10.5194/acp-2021-8
Preprint. Discussion started: 29 January 2021


Atmospheric Chemistry and Physics Discussions

3.2 In-depth investigation of periods with high organic aerosol mass loadings (13th -18th of May)

As pointed out above, high aerosol particle loadings occurred between May 13 and 18. An in-depth analysis of the aerosol particle composition and volatility is performed in this section for this noteworthy period. Three distinct sub-periods were chosen, involving times when monoterpene oxidation products were dominating over sesquiterpene products (event A), when sesquiterpene oxidation products were prevailing (event B), and when their concentrations were similar (event C) (Fig. 4). The single measurement cycles corresponding to the concentration maximums of each event were used for the referred analysis.

3.2.1 Early morning concentration maxima of sesquiterpene oxidation products

We looked in more detail at the time series of the presumed monoterpene and sesquiterpene oxidation products, as measured by FIGAERO-CIMS, during the period from 13th to 18th of May, including a comparison with concomitant measurements of precursor VOCs by PTR-ToF-MS, O_3 concentrations, air temperature, PAR and mixing height (Fig. 5; the same overview is shown for the whole campaign period in Fig. S5). For both monoterpenes and sesquiterpenes, a distinct diel pattern was observed (Fig. 6), somewhat similar to that of the aerosol particle mass loading (e.g. Fig. 5). The concentrations of these terpene classes started to increase during the evening (between 19h-22h). This increase was driven by changes in both boundary layer and chemistry, since the mixing height decreases after sunset and enhances the reactivity between concentrated BVOCs and atmospheric oxidants (Praplan et al., 2019). The nocturnal decrease in mixing height also affects near-surface aerosol loadings. The particle phase concentrations of monoterpene oxidation products increased with monoterpene concentrations, revealing the importance of night-time oxidation for the formation of condensable vapors from monoterpenes. Furthermore, decreasing temperatures during night-time enhance the partitioning of oxidation products from gas to particle phase (Li et al., 2019b). However, decoupling this range of concurring chemical, physical and meteorological mechanisms driving the overall SOA loadings is beyond the scope of our study.

The increase in monoterpenes was often followed by an increase in sesquiterpene amounts (Fig. S5), suggesting that they were subjected to similar sources and sinks for most time periods. Interestingly, unlike for the monoterpenes, the maxima of sesquiterpene concentrations were observed consistently around 6 am between 13th and 18th of May (Fig. 6). We are unaware of previously published observations of this phenomenon, although a dataset from a recent study of terpenes in the French Landes forest may suggest an increase in sesquiterpene emissions during early July mornings as well (Li et al., 2020a). In our study, we observed sesquiterpene spikes during many mornings from May 6 until a break in PTR-ToF-MS measurements on May 21, so these spikes may be a common phenomenon possibly related to a certain plant phase in spring. A possible reason for the general increase in sesquiterpene emissions observed in May could be related to plant growth. Nemecek-Marshall et al. (1995) have found morning emission bursts of methanol that were related to the leaf growth. Jardine et al. (2016) have also reported methanol and isoprene emissions related to growth processes from Amazonian tree species. Therefore, sesquiterpene emissions resulting from plant growth are also possible, especially since plant growth at the measurement site usually occurs during morning hours in mid-May. Since sesquiterpenes have higher Henry´s law constant than monoterpenes (Copolovici

https://doi.org/10.5194/acp-2021-8
Preprint. Discussion started: 29 January 2021


Atmospheric Chemistry and Physics Discussions

and Niinemets, 2015), one could also speculate that they are more efficiently retained in plants or on surfaces under stagnant nocturnal conditions, which might then trigger a more pronounced increase in concentrations at some distance from the canopy space (and to the PTR-ToF-MS inlet). The increase in sesquiterpenes coincided with the minimum in O_3 concentration. In a study performed at a boreal forest site in Hyytiälä, Finland, Hellén et al. (2018) showed that, whereas the chemistry of monoterpenes is dominated by reactions with OH and NO_3 radicals, sesquiterpenes react mostly with O_3. Thus, the minimum in O_3 concentrations may enhance the sesquiterpene concentration more strongly than the monoterpenes one during the time around sunset.

The peak concentrations of particulate o-SQT compounds aligned with the maxima in sesquiterpene concentrations and dips in O_3 levels, occurring later than the peak for o-MT compounds. This practically immediate response of SOA particle loading and composition to sesquiterpene emissions reveals the importance of sesquiterpenes to SOA and broadly verifies the classification applied in this study. The concentrations of o-highH1 and o-highH2 were increasing simultaneously with o-SQT, which suggests that these groups correspond at least partially to sesquiterpene oxidation products (either actually or resulting from misidentifying chemical formulas; Sect. S5 and Fig. S6 in the supplement material). For that reason, it is likely that the particle phase concentration of sesquiterpene oxidation products, and hence their contribution to the SOA particle composition, are still underestimated in this study. Similarly, Dimers followed the concentrations of presumable sesquiterpene oxidation products as well. Since this group may include diterpene oxidation products, it is possible that these compounds were produced by similar processes as the sesquiterpene oxidation products. However, misidentification in detriment of sesquiterpene oxidation products is possible for this group of compounds as well.

A comparison between isoprene measured by PTR-ToF-MS and o-$C_{4\text{-}5}$ was also performed, as most condensed isoprene oxidation products are expected to be found as o-$C_{4\text{-}5}$. The o-$C_{4\text{-}5}$ increased with isoprene concentrations, at least during the 13th to 18th of May period (Fig. S5). Isoprene and o-$C_{4\text{-}5}$ were high during the event A when o-MT dominated, but were low during the sesquiterpene event B. However, this group can significantly include decomposition products of both o-MT and o-SQT and for that reason the contribution of isoprene oxidation to the observed events cannot be determined with the methodology of this study.

3.2.2 Relative contributions of the different terpene oxidation product groups

During the selected events, the most significant contributions to organic aerosol particulate mass were derived from monoterpenes and sesquiterpenes, least ambiguously associated with the o-MT and o-SQT groups, respectively (Fig. 5). The relative significance of these groups was evaluated by dividing the corresponding concentrations by the total sum of these two groups. In event A, the contribution of o-MT relatively to o-SQT was clearly higher, with a percentage of 83 %. However, this contribution changed significantly during event B when the o-SQT relative contribution increased sharply, from 17 % to 66 %. The levels of these two groups of oxidation products were similar in event C, with 56 % of o-MT and 44 % of o-SQT. The o-highH1 and o-highH2 concentrations increased during event B and were lower during event A, also suggesting that at least

https://doi.org/10.5194/acp-2021-8
Preprint. Discussion started: 29 January 2021


Atmospheric Chemistry and Physics Discussions

some of the analytes in these groups stem from sesquiterpene oxidation (see Sect. 3.2.1 and S5). On the other hand, the changes in contribution from the groups ON, o-$C_{4\text{-}5}$ and Others were less significant between events.

The contribution of monoterpene and sesquiterpene oxidation products to SOA particles was mostly dominated by only a few chemical formulas (Fig. 7, note that this analysis assumes that all analytes have similar instrument sensitivity (see Sect. 2)). For o-SQT, the 10 most abundant chemical formulas constituted 58.7 % to 65.3 % of the total concentration of these oxidation products in SOA particles (109 chemical formulas identified in total) during events A-C, with higher contributions during events B and C when the total concentrations of sesquiterpene products were also higher. For o-MT, the 10 dominant chemical formulas contributed about 40 % to the sum of o-MT products by mass (170 different chemical formulas in total), with a higher percentage of 46.6 % being observed during event A when the monoterpene oxidation products prevailed.

Another interesting observation is that most of the 10 prevailing o-MT and o-SQT were present in all three events on May 15, 17 and 18, although the particles were formed on different days and consequently under slightly different atmospheric conditions and reactant concentrations (see e.g. Fig. 5 and Fig. S2). Apparently, those specific products (presented in Fig. 7) have either a particularly high atmospheric production or a high tendency to partition form the gas to particle phase, or both. This observation particularly applies to the sesquiterpene products, as the relative contribution of the 10 most abundant chemical formulas was higher for o-SQT than for o-MT. This result is somewhat unexpected since, generally, the structural diversity of sesquiterpenes exceeds that of monoterpenes due to the many more types of cyclization that are possible with the five additional carbon atoms (Langenheim, 2003). However, the actual structure of the terpenes may also play an important role, since e.g. cyclic terpenes have been shown to produce more SOA than acyclic ones (e.g. Ylisirniö et al., 2020a).

The o-SQT that contributed the most to the aerosol particle composition were $C_{15}H_{24}O_3$ and $C_{14}H_{22}O_4$. These compounds have been identified as the major primary oxidation products formed from β-caryophyllene ozonolysis in a laboratory study performed under atmospherically relevant conditions (Li et al., 2011). Gas phase samples at our sampling site suggested that the most abundant sesquiterpene specie during the sesquiterpene event B was longifolene-(V4) (Fig. S2). Note, however, that these GC-MS terpene speciation measurements used 30 minutes collections of VOCs at varying times of day, whereas our defined events (A, B, C) all occurred during night-time/early morning. Also, no VOC samples were collected for GC-MS analysis during the actual day of event B (May 17). The species formed during atmospheric oxidative reactions of longifolene-(V4) are currently unknown but, with its cyclic structure and endocyclic double bond, products similar to those from β-caryophyllene might be formed. Interestingly, $C_{15}H_{24}O_3$ seemed to have a particularly important role in the increase of sesquiterpene-dominated SOA particulate mass, since its relative contribution was highest during the sesquiterpene event B.

Among the monoterpene oxidation products, $C_8H_{12}O_5$ and $C_7H_{10}O_5$ were the dominant ones for all three investigated periods. These compounds have been found in another study performed at a boreal forest site in Hyytiälä, Finland, by employing the same method of FIGAERO-I-CIMS (Lee et al., 2018). Both products have been also found in controlled laboratory studies on the oxidation of monoterpene species using FIGAERO-CIMS, such as from limonene (Hammes et al., 2019), α-pinene (D'Ambro et al., 2018), or Δ^3-carene (Li et al., 2020b).

https://doi.org/10.5194/acp-2021-8
Preprint. Discussion started: 29 January 2021


Atmospheric Chemistry and Physics Discussions

3.2.3 Comparison between FIGAERO-CIMS results and off-line measurements by GC-QToF-MS and LC-QToF-MS

Off-line filter measurements of OA particle composition were also performed with GC-QToF-MS and LC-QToF-MS. Since iodide ionization was used for the CIMS measurements and aerosol particle phase constituents generally have low vapor pressures, the obtained results with FIGAERO-CIMS are expected to be most comparable with those obtained by LC-QToF-MS in negative ionization mode. However, LC-QToF-MS measurements performed in positive mode and GC-QToF-MS measurements performed in negative mode were also included in this study since they could contribute to understanding the potential presence of SOA constituents that FIGAERO-CIMS might not be sensitive to.

Figure 8 gives an overview of the chemical composition measured by the three techniques employed in this study for the chemical characterization of the OA particle phase. The focus was on events A (o-MT dominant) and B (o-SQT dominant) and compounds were grouped as before (Table 1). A change in the proportional contributions of the groups was observed between the different techniques. FIGAERO-CIMS and LC-QToF-MS (negative mode) seemed to be particularly sensitive to the o-MT and o-SQT products during the periods when the corresponding terpene concentrations increased. On the other hand, LQ-QToF-MS (positive mode) was more sensitive to organonitrates and dimers, since their fraction was the highest from all methods in both events. The o-MT greatly dominated the terpenoid PM_1 fraction measured by GC-QToF-MS (negative mode), suggesting a higher volatility of o-MT when compared to o-SQT products. These results show the importance of employing different analytical methods for a comprehensive characterization of aerosol particle composition.

Similar to what was observed for the FIGAERO-CIMS measurements, the presumed sesquiterpene oxidation products increased in event B for the LC-QToF-MS measurements in positive and negative mode (Fig. S7; period 11/5-15/5 for event A, period 15/5-19/5 for event B). For GC-QToF-MS, the opposite was observed, which might be explained by the fact that this technique is not suitable for the analysis of larger oxygenated compounds due to their low vapor pressures. Since the partitioning into the particle phase is enhanced by the decrease in organics vapor pressure and the investigation of the organic compounds contributing to aerosol particles was the aim of our study, we focus on the results from the FIGAERO-CIMS and LC-QToF-MS that will detect the majority of these less volatile compounds. The o-highH1 analytes were not found in off-line samples, while the o-highH2 ones were only found in the LC-QToF-MS measurements. This result supports the notion that a significant fraction of these analytes might be misidentified o-SQT compounds or were created in the thermal desorption process. As explained above, such misidentification could have been a result from an insufficient resolution of the HR-ToF-CIMS for high m/z ions (e.g. Fig. S6). The use of chromatographic separation and truly higher resolution instrumentation, such as the LC-QToF-MS used in this study, can possibly provide better chemical formula identification. However, off-line techniques are also prone to sample modification, i.e., the analytes might have suffered chemical decomposition/losses during sample preparation/storage. The most dominant compounds measured by LC-QToF-MS and GC-QToF-MS during the periods when events A and B occurred are presented in Figs. S8 and S9. A comparison of those compositions with the ones obtained from FIGAERO-CIMS is discussed in Sect. S6.

https://doi.org/10.5194/acp-2021-8
Preprint. Discussion started: 29 January 2021


Atmospheric Chemistry and Physics Discussions

3.2.4 Organic aerosol particle volatility

Particle phase analytes were classified according to their volatility (expressed as C^*, in µg m^{-3}) as volatile organic compounds (VOC), intermediate volatile organic compounds (IVOC), semi-volatile organic compounds (SVOC), low volatile organic compounds (LVOC) and extremely low volatile organic compounds (ELVOC), following the criteria described in Donahue et al. (2012). C^* values were derived using two different methods, one method based on the assigned elemental composition and another based on the measured thermograms (see Sect. 2.3). When deriving C^* purely from the assigned elemental compositions (Eq. (3); Li et al., 2016), the majority of measured SOA particle constituents were classified as SVOCs and IVOCs (Fig. 9, left), whereas when C^* was derived from thermograms a clear dominance of LVOCs was observed (Fig. 9, center) with very little contribution from SVOCs and ELVOCs. Since the thermograms reflect the volatility of aerosol composition based on their volatilization from the aerosol state (Lopez-Hilfiker et al., 2014), the thermogram-based method constitutes a more direct and realistic approach for determining C^*, especially since thermal decomposition likely plays a significant role (Lopez-Hilfiker et al., 2015; Schobesberger et al., 2018). Thermal decomposition will lead to the detection of fragments of the original molecule. The parameterization method will then be likely to assign a higher volatility C^* to these fragments than that derived from their thermograms. For the same reason, the C^* value derived from the thermogram will also tend to be higher than the true volatility of the decomposing compound, but it will be closer to the true value than the one derived from the composition of a much smaller molecule fragment.

The ELVOC fraction was low in this study when compared to LVOC, also when considering the thermogram-based results. However, the following issues may cause a bias towards higher volatilities in FIGAERO-CIMS thermogram-based methods. First (a), aerosol chemical desorption may be limited by the maximum temperature reached by FIGAERO, i.e., eventually the applied thermal energy may be insufficient for the desorption of ELVOC from the particles collected on the filter into the analytical instrument. Also (b), the less volatile a compound is, the more likely it is generally to thermally decompose prior to evaporation. The same applies for increasingly functionalized organic compounds, the major cause for the low volatility of ELVOCs. Another issue (c) may be within the method itself. When determining T_{max} values, it is assumed that each chemical formula represents a single compound whose volatility is described by the T_{max} value. But it has been shown that there can be multiple isomers with different volatilities, creating multi-modal or broad thermograms (Lopez-Hilfiker et al., 2014; Schobesberger et al., 2018). Such isomers may evaporate or decompose at desorption temperatures different from the pronounced T_{max} value. Their systematic omission by the T_{max} method (Fig. 9, center) is avoided if T_{max} are ignored and the full desorption temperature axis of the total thermogram, summed over all chemical formulas, is simply translated to a C^* axis using Eq. (1) (inserting desorption temperature instead of T_{max}; Fig. 9, right). The resulting volatility distribution is substantially broader, with the concentration-weighted C^* shifting to lower volatilities. This method deals with issue (c), but as thermogram peak shapes are now ignored, biases are potentially added at both low and high volatilities, while potential high biases due to insufficient temperature (a) or due to decomposition occurring prior to evaporation (b) are still not dealt with.

https://doi.org/10.5194/acp-2021-8
Preprint. Discussion started: 29 January 2021


Atmospheric Chemistry and Physics Discussions

The extension of fragmentation and its influence on volatility was evaluated by comparing some thermograms in more detail, namely the sum of constituents with different oxygen content (3 to ≥7) and the corresponding dominant signals contributing to the groups of presumed monoterpene and sesquiterpene oxidation products (groups o-MT and o-SQT, respectively; Fig. 10). The thermograms from o-MT seemed to exhibit more broadening compared to o-SQT, likely indicating a larger influence of thermal decomposition on the measured signals. The occurrence of thermal decomposition could contribute to higher T_{max}, despite lower #C. But in the investigated cases, the change in the detailed peak shape (i.e. the degree of broadening or the peak to tail ratio) did not impact greatly on the T_{max} values. Overall, the T_{max} was increasing with the increase in oxygen content as expected for oxygen-containing functional groups, which generally decreases the volatility of a compound. Between the different events, the T_{max} of the presented ion thermograms were similar, but the importance of the peak tail varied significantly. Interestingly, the thermogram-based volatility was higher during the o-SQT event B. This result may be explained by the low aging of o-SQT products comparatively to the ones from monoterpenes (Fig. 9). A more detailed look into composition- and thermogram-derived volatilities is provided in the supplement, where Fig. S10 gives an overview of the range of identified chemical formulas and their C^* derived with both methods. It also explores the influence of the O:C ratio on volatility during the different events. A significant fraction of the most dominant constituents had an O:C ratio between 0.5 and 1 during event A and B when monoterpene and sesquiterpene oxidation products dominated aerosol composition, respectively. However, during event B, an increase in C_{15} analytes with lower O:C was observed, again suggesting the increased contribution of more recently formed (hence less oxygenated) sesquiterpene oxidation products. As expected from the results in Fig. 10, some trends in volatility follow expectations from the observed compositions, also for the thermogram-based C^* although they are lower throughout. The plots also indicate generally high T_{max} for small compounds (for example with #C < 5), which is a strong evidence for thermal decomposition as the origin of those analytes.

4 Conclusions

In this study, organic analytes were successfully measured on-line at a hemi-boreal forest by FIGAERO-CIMS. The study led to a comprehensive characterization of the organic aerosol chemical composition at the measurement site. A range of terpene oxidation products were identified both in the gas and particle phase. The highest SOA particle loadings occurred typically during night-time and early morning. Monoterpenes and sesquiterpenes were the main precursors to SOA particles, with mean concentrations for arguably monoterpene-derived (o-MT) and sesquiterpene-derived products (o-SQT) of 0.4 and 0.1 μg m^{-3}, respectively. Even though the concentration of sesquiterpene oxidation products was low in the gas phase throughout the campaign, with mean concentrations of 0.07 μg m^{-3}, they were important contributors to the aerosol particle phase during certain periods of time with maximum particle phase concentrations of 1.6 μg m^{-3}. The practically immediate presence of these products in SOA particles upon the early morning maximum in sesquiterpene gas phase concentrations suggested their fast partitioning into the particle phase. The sesquiterpene products concentration in aerosol particles exceeded that of monoterpene oxidation products at some of those occasions. These findings are supported by chromatography-mass spectrometry off-line

https://doi.org/10.5194/acp-2021-8
Preprint. Discussion started: 29 January 2021


Atmospheric Chemistry and Physics Discussions

measurements that provided precursor VOC speciation and higher-resolution mass spectra of aerosol particle composition. An interesting phenomenon observed in this study was the presence of marked maxima in sesquiterpene mixing ratios in the early mornings, with increases starting at sunrise and ultimate decreases due to the onset of daytime convective mixing. Future studies are needed to elucidate the mechanism behind these increases in sesquiterpene mixing ratios. A combination of (a) an increase in specific plant emissions, (b) mixing-enhanced release from canopy storage, and (c) a particularly supressed oxidation rate by O_3 depletion might explain the observed phenomenon.

More detailed analysis of the particle phase composition and volatility gave additional indications that the observed sesquiterpene oxidation products are rapidly formed in significant amounts. Their relatively low O:C ratios also suggest that they have not been highly processed. It is plausible that a recent atmospheric formation is responsible for the relatively higher volatility of those products in our observations compared to the one from monoterpene products, whereas it is unlikely that particle phase organic material that originates from sesquiterpene oxidation would generally be more volatile than material originating from monoterpene oxidation. A consequent conclusion would be that sesquiterpene-sourced SOA material may soon become unrecognizable as such, i.e., that aging may make that material undistinguishable from aged monoterpene SOA. However, the oxidation products formed are highly dependent on the original terpene structure.

Altogether, our results support a substantial contribution of sesquiterpenes to hemi-boreal SOA during spring-time, suggesting that both atmospheric measurements and models that focus on monoterpene oxidation may overlook a potentially large fraction of SOA particulate mass. We also saw evidence of the importance of considering the molecular structure of the involved terpenes on SOA formation instead of only their terpene class, as recently reported, e.g., by Ylisirniö et al. (2020a). Clearly, more detailed and systematic studies are warranted to investigate the formation of SOA from the oxidation of a variety of sesquiterpenes, and how sesquiterpene emissions vary both quantitatively (e.g., diel variations) and qualitatively (e.g., relative contributions of cyclic vs. acyclic species). The detailed chemical analysis of the expected range of particle phase material would benefit greatly from the use of even higher resolution techniques and chromatographic methods since the compound separation and identification with the HR-ToF-CIMS employed here was challenging and, as demonstrated, substantial ambiguities have remained. In addition, future studies of ambient SOA using FIGAERO-CIMS (including the dataset obtained here) will likely benefit from the currently on-going development of techniques to deconvolute and interpret thermogram data sets (Buchholz et al., 2020).

Data availability. The data shown in the paper is available on request from corresponding author.

Author contribution. LB, AY, IP, HL, HJ, SN, AK, DK, KK, ET, UN and SS carried the experiments. LB, AY, IP, AB, ZL, HL, HJ, SN, AK, DK, KK, ET, UN, JRJ and SS contributed to the data analysis and interpretation. HJ, SN and SS contributed to the funding acquisition and supervision. LB wrote the manuscript. All authors participated to the interpretation of the results and paper editing.

https://doi.org/10.5194/acp-2021-8
Preprint. Discussion started: 29 January 2021


Atmospheric Chemistry and Physics Discussions

Competing interests. The authors declare that they have no conflict of interest.

Acknowledgements. This research was supported by the Academy of Finland (310682). We appreciate Biocentre Finland and Biocentre Kuopio for supporting LC-MS laboratory facility. We acknowledge Prof. Marja-Liisa Riekkola from the Department of Chemistry of University of Helsinki for the possibility to use the GC-QToF-MS. SN acknowledges support from the European network for observing our changing planet project (ERA-PLANET, grant agreement no. 689443) under the European Union's Horizon 2020 research and innovation programme and the Estonian Ministry of Sciences projects (grant nos. P180021, P180274), the Estonian Research Infrastructures Roadmap project Estonian Environmental Observatory (3.2.0304.11-0395), and the European Commission through the European Regional Fund (the Centre of Excellence ENVIRON).

References

Atkinson, R. and Arey, J.: Gas-phase tropospheric chemistry of biogenic volatile organic compounds: a review, Atmos. Environ., 37, 197–219, doi:10.1016/S1352-2310(03)00391-1, 2003.

Barreira, L. M. F., Helin, A., Aurela, M., Teinilä, K., Friman, M., Kangas, L., Niemi, J. V., Portin, H., Kousa, A., Pirjola, L., Rönkkö, T., Saarikoski, S. and Timonen, H.: In-depth characterization of submicron particulate matter inter-annual variations at a street canyon site in Northern Europe, Atmos. Chem. Phys. Discuss., 1–34, doi:10.5194/acp-2020-908, 2020.

Buchholz, A., Ylisirniö, A., Huang, W., Mohr, C., Canagaratna, M., Worsnop, D. R., Schobesberger, S. and Virtanen, A.: Deconvolution of FIGAERO–CIMS thermal desorption profiles using positive matrix factorisation to identify chemical and physical processes during particle evaporation, Atmos. Chem. Phys., 20(13), 7693–7716, doi:10.5194/acp-20-7693-2020, 2020.

Copolovici, L. and Niinemets, Ü.: Temperature dependencies of Henry's law constants for different plant sesquiterpenes, Chemosphere, 138, 751–757, doi:10.1016/j.chemosphere.2015.07.075, 2015.

D'Ambro, E. L., Schobesberger, S., Zaveri, R. A., Shilling, J. E., Lee, B. H., Lopez-Hilfiker, F. D., Mohr, C. and Thornton, J. A.: Isothermal Evaporation of α-Pinene Ozonolysis SOA: Volatility, Phase State, and Oligomeric Composition, ACS Earth Space Chem., 2(10), 1058–1067, doi:10.1021/acsearthspacechem.8b00084, 2018.

Donahue, N. M., Epstein, S., Pandis, S. N. and Robinson, A. L.: A two-dimensional volatility basis set: 1. organic-aerosol mixing thermodynamics, Atmos. Chem. Phys., 11(7), 3303–3318, doi:10.5194/acp-11-3303-2011, 2011.

Donahue, N. M., Kroll, J., Pandis, S. N. and Robinson, A. L.: A two-dimensional volatility basis set–Part 2: Diagnostics of organic-aerosol evolution, Atmos. Chem. Phys., 12(2), 615–634, doi:10.5194/acp-12-615-2012, 2012.

Duporté, G., Parshintsev, J., Barreira, L. M., Hartonen, K., Kulmala, M. and Riekkola, M.-L.: Nitrogen-containing low volatile compounds from pinonaldehyde-dimethylamine reaction in the atmosphere: A laboratory and field study, Environ. Sci. Technol., 50(9), 4693–4700, doi:10.1021/acs.est.6b00270, 2016.

Ezhova, E., Ylivinkka, I., Kuusk, J., Komsaare, K., Vana, M., Krasnova, A., Noe, S., Arshinov, M., Belan, B., Park, S.-B., Lavrič, J. V., Heimann, M., Petäjä, T., Vesala, T., Mammarella, I., Kolari, P., Bäck, J., Rannik, Ü., Kerminen, V.-M. and

Kulmala, M.: Direct effect of aerosols on solar radiation and gross primary production in boreal and hemiboreal forests, Atmos. Chem. Phys., 18(24), 17863–17881, doi:10.5194/acp-18-17863-2018, 2018.

Fraser, M. P. and Lakshmanan, K.: Using Levoglucosan as a Molecular Marker for the Long-Range Transport of Biomass Combustion Aerosols, Environ. Sci. Technol., 34(21), 4560–4564, doi:10.1021/es991229l, 2000.

Grote, R., Monson, R. K. and Niinemets, Ü.: Leaf-Level Models of Constitutive and Stress-Driven Volatile Organic Compound Emissions, in Niinemets Ü., Monson R. (eds) Biology, Controls and Models of Tree Volatile Organic Compound Emissions, Tree Physiology, vol 5, Springer, Dordrecht, 10.1007/978-94-007-6606-8_12., 2013.

Guenther, A., Hewitt, C. N., Erickson, D., Fall, R., Geron, C., Graedel, T. and McKay, W.: A global model of natural volatile organic compound emissions, J. Geophys. Res. Atmos., 100(D5), 8873–8892, doi:10.1029/94JD02950, 1995.

Hallquist, M., Wenger, J. C., Baltensperger, U., Rudich, Y., Simpson, D., Claeys, M. and Goldstein, A.: The formation, properties and impact of secondary organic aerosol: current and emerging issues, Atmos. Chem. Phys., 9(14), 5155–5236, doi:10.5194/acp-9-5155-2009, 2009.

Hammes, J., Lutz, A., Mentel, T., Faxon, C. and Hallquist, M.: Carboxylic acids from limonene oxidation by ozone and hydroxyl radicals: insights into mechanisms derived using a FIGAERO-CIMS, Atmos. Chem. Phys., 19(20), 13037–13052, doi:10.5194/acp-19-13037-2019, 2019.

Hao, L., Garmash, O., Ehn, M., Miettinen, P., Massoli, P., Mikkonen, S., Jokinen, T., Roldin, P., Aalto, P., Yli-Juuti, T., Joutsensaari, J., Petäjä, T., Kulmala, M., Lehtinen, K. E. J., Worsnop, D. R. and Virtanen, A.: Combined effects of boundary layer dynamics and atmospheric chemistry on aerosol composition during new particle formation periods, Atmos. Chem. Phys., 18(23), 17705–17716, doi:10.5194/acp-18-17705-2018, 2018.

Helin, A., Niemi, J. V., Virkkula, A., Pirjola, L., Teinilä, K., Backman, J., Aurela, M., Saarikoski, S., Rönkkö, T., Asmi, E. and Timonen, H.: Characteristics and source apportionment of black carbon in the Helsinki metropolitan area, Finland, Atmos. Environ., 190, 87–98, doi:10.1016/j.atmosenv.2018.07.022, 2018.

Hellén, H., Praplan, A. P., Tykkä, T., Ylivinkka, I., Vakkari, V., Bäck, J., Petäjä, T., Kulmala, M. and Hakola, H.: Long-term measurements of volatile organic compounds highlight the importance of sesquiterpenes for the atmospheric chemistry of a boreal forest, Atmos. Chem. Phys., 18(19), 13839–13863, doi:10.5194/acp-18-13839-2018, 2018.

Iyer, S., Lopez-Hilfiker, F., Lee, B. H., Thornton, J. A. and Kurtén, T.: Modeling the Detection of Organic and Inorganic Compounds Using Iodide-Based Chemical Ionization, J. Phys. Chem. A, 120(4), 576–587, doi:10.1021/acs.jpca.5b09837, 2016.

Jardine, K. J., Jardine, A. B., Souza, V. F., Carneiro, V., Ceron, J. V., Gimenez, B. O., Soares, C. P., Durgante, F. M., Higuchi, N., Manzi, A. O., Gonçalves, J. F. C., Garcia, S., Martin, S. T., Zorzanelli, R. F., Piva, L. R. and Chambers, J. Q.: Methanol and isoprene emissions from the fast growing tropical pioneer species Vismia guianensis (Aubl.) Pers. (Hypericaceae) in the central Amazon forest, Atmos. Chem. Phys., 16(10), 6441–6452, doi:10.5194/acp-16-6441-2016, 2016.

Joensuu, J., Altimir, N., Hakola, H., Rostás, M., Raivonen, M., Vestenius, M., Aaltonen, H., Riederer, M. and Bäck, J.: Role of needle surface waxes in dynamic exchange of mono- and sesquiterpenes, Atmos. Chem. Phys., 16(12), 7813–7823, doi:10.5194/acp-16-7813-2016, 2016.

Jokinen, T., Berndt, T., Makkonen, R., Kerminen, V.-M., Junninen, H., Paasonen, P., Stratmann, F., Herrmann, H., Guenther, A. B., Worsnop, D. R., Kulmala, M., Ehn, M. and Sipilä, M.: Production of extremely low volatile organic compounds from

biogenic emissions: Measured yields and atmospheric implications, Proc. Natl. Acad. Sci. USA, 112(23), 7123–7128, doi:10.1073/pnas.1423977112, 2015.

Junninen, H., Ehn, M., Petäjä, T., Luosujärvi, L., Kotiaho, T., Kostiainen, R. and Kulmala, M.: A high-resolution mass spectrometer to measure atmospheric ion composition, Atmos. Meas. Tech., 3(4), 1039–1053, doi:10.5194/amt-3-1039-2010, 2010.

Kännaste, A., Copolovici, L. and Niinemets, Ü.: Gas Chromatography–Mass Spectrometry Method for Determination of Biogenic Volatile Organic Compounds Emitted by Plants, in Rodríguez-Concepción M. (eds) Plant Isoprenoids. Methods in Molecular Biology (Methods and Protocols), vol 1153. Humana Press, New York, NY. https://doi.org/10.1007/978-1-4939-0606-2_11., 2014.

Kansal, A.: Sources and reactivity of NMHCs and VOCs in the atmosphere: A review, J. Hazard. Mater., 166(1), 17–26, doi:10.1016/j.jhazmat.2008.11.048, 2009.

Kari, E., Faiola, C. L., Isokääntä, S., Miettinen, P., Yli-Pirilä, P., Buchholz, A., Kivimäenpää, M., Mikkonen, S., Holopainen, J. K. and Virtanen, A.: Time-resolved characterization of biotic stress emissions from Scots pines being fed upon by pine weevil by means of PTR-ToF-MS, Boreal Env. Res., 24, 25–49, 2019.

Kavouras, I. G., Mihalopoulos, N. and Stephanou, E.: Formation and gas/particle partitioning of monoterpenes photo-oxidation products over forests, Geophys. Res. Lett., 26(1), 55–58, doi:10.1029/1998GL900251, 1999.

Langenheim, J. H.: Plant resins: chemistry, evolution, ecology, and ethnobotany, Oregon, US: Timber Press., 2003.

Laothawornkitkul, J., Taylor, J. E., Paul, N. D. and Hewitt, C. N.: Biogenic volatile organic compounds in the Earth system, New Phytol., 183(1), 27–51, doi:10.1111/j.1469-8137.2009.02859.x, 2009.

Lee, B. H., Lopez-Hilfiker, F. D., Mohr, C., Kurtén, T., Worsnop, D. R. and Thornton, J. A.: An iodide-adduct high-resolution time-of-flight chemical-ionization mass spectrometer: Application to atmospheric inorganic and organic compounds, Environ. Sci. Technol., 48(11), 6309–6317, doi:10.1021/es500362a, 2014.

Lee, B. H., Lopez-Hilfiker, F. D., D'Ambro, E. L., Zhou, P., Boy, M., Petäjä, T., Hao, L., Virtanen, A. and Thornton, J. A.: Semi-volatile and highly oxygenated gaseous and particulate organic compounds observed above a boreal forest canopy, Atmos. Chem. Phys., 18(15), 11547–11562, doi:10.5194/acp-18-11547-2018, 2018.

Lehtipalo, K., Yan, C., Dada, L., Bianchi, F., Xiao, M., Wagner, R., Stolzenburg, D., Ahonen, L. R., Amorim, A., Baccarini, A., Bauer, P. S., Baumgartner, B., Bergen, A., Bernhammer, A.-K., Breitenlechner, M., Brilke, S., Buchholz, A., Mazon, S. B., Chen, D., Chen, X., Dias, A., Dommen, J., Draper, D. C., Duplissy, J., Ehn, M., Finkenzeller, H., Fischer, L., Frege, C., Fuchs, C., Garmash, O., Gordon, H., Hakala, J., He, X., Heikkinen, L., Heinritzi, M., Helm, J. C., Hofbauer, V., Hoyle, C. R., Jokinen, T., Kangasluoma, J., Kerminen, V.-M., Kim, C., Kirkby, J., Kontkanen, J., Kürten, A., Lawler, M. J., Mai, H., Mathot, S., Mauldin, R. L., Molteni, U., Nichman, L., Nie, W., Nieminen, T., Ojdanic, A., Onnela, A., Passananti, M., Petäjä, T., Piel, F., Pospisilova, V., Quéléver, L. L. J., Rissanen, M. P., Rose, C., Sarnela, N., Schallhart, S., Schuchmann, S., Sengupta, K., Simon, M., Sipilä, M., Tauber, C., Tomé, A., Tröstl, J., Väisänen, O., Vogel, A. L., Volkamer, R., Wagner, A. C., Wang, M., Weitz, L., Wimmer, D., Ye, P., Ylisirniö, A., Zha, Q., Carslaw, K. S., Curtius, J., Donahue, N. M., Flagan, R. C., Hansel, A., Riipinen, I., Virtanen, A., Winkler, P. M., Baltensperger, U., Kulmala, M. and Worsnop, D. R.: Multicomponent new particle formation from sulfuric acid, ammonia, and biogenic vapors, Sci. Adv., 4(12), eaau5363, doi:10.1126/sciadv.aau5363, 2018.

Li, H., Riva, M., Rantala, P., Heikkinen, L., Daellenbach, K., Krechmer, J. E., Flaud, P.-M., Worsnop, D., Kulmala, M., Villenave, E., Perraudin, E., Ehn, M. and Bianchi, F.: Terpenes and their oxidation products in the French Landes forest:

insights from Vocus PTR-TOF measurements, Atmos. Chem. Phys., 20(4), 1941–1959, doi:10.5194/acp-20-1941-2020, 2020a.

Li, X., Chee, S., Hao, J., Abbatt, J. P. D., Jiang, J. and Smith, J. N.: Relative humidity effect on the formation of highly oxidized molecules and new particles during monoterpene oxidation, Atmos. Chem. Phys., 19(3), 1555–1570, doi:10.5194/acp-19-1555-2019, 2019a.

Li, Y., Chen, Q., Guzman, M., Chan, C. and Martin, S.: Second-generation products contribute substantially to the particle-phase organic material produced by β-caryophyllene ozonolysis, Atmos. Chem. Phys., 11(1), 121–132, doi:10.5194/acp-11-121-2011, 2011.

Li, Y., Pöschl, U. and Shiraiwa, M.: Molecular corridors and parameterizations of volatility in the chemical evolution of organic aerosols, Atmos. Chem. Phys., 16(5), 3327–3344, doi:10.5194/acp-16-3327-2016, 2016.

Li, Z., Tikkanen, O.-P., Buchholz, A., Hao, L., Kari, E., Yli-Juuti, T. and Virtanen, A.: Effect of Decreased Temperature on the Evaporation of α-Pinene Secondary Organic Aerosol Particles, ACS Earth Space Chem., 3(12), 2775–2785, doi:10.1021/acsearthspacechem.9b00240, 2019b.

Li, Z., D'Ambro, E. L., Schobesberger, S., Gaston, C. J., Lopez-Hilfiker, F. D., Liu, J., Shilling, J. E., Thornton, J. A. and Cappa, C. D.: A robust clustering algorithm for analysis of composition-dependent organic aerosol thermal desorption measurements, Atmos. Chem. Phys., 20(4), 2489–2512, doi:10.5194/acp-20-2489-2020, 2020b.

Lopez-Hilfiker, F., Mohr, C., Ehn, M., Rubach, F., Kleist, E., Wildt, J. and Worsnop, D.: A novel method for online analysis of gas and particle composition: description and evaluation of a Filter Inlet for Gases and AEROsols (FIGAERO), Atmos. Meas. Tech., 7(4), 983–1001, doi:10.5194/amt-7-983-2014, 2014.

Lopez-Hilfiker, F. D., Mohr, C., Ehn, M., Rubach, F., Kleist, E., Wildt, J., Mentel, T. F., Carrasquillo, A. J., Daumit, K. E., Hunter, J. F., Kroll, J. H., Worsnop, D. R. and Thornton, J. A.: Phase partitioning and volatility of secondary organic aerosol components formed from α-pinene ozonolysis and OH oxidation: the importance of accretion products and other low volatility compounds, Atmos. Chem. Phys., 15(14), 7765–7776, doi:10.5194/acp-15-7765-2015, 2015.

Lopez-Hilfiker, F. D., Iyer, S., Mohr, C., Lee, B. H., D'Ambro, E. L., Kurtén, T. and Thornton, J. A.: Constraining the sensitivity of iodide adduct chemical ionization mass spectrometry to multifunctional organic molecules using the collision limit and thermodynamic stability of iodide ion adducts, Atmos. Meas. Tech., 9(4), 1505–1512, doi:10.5194/amt-9-1505-2016, 2016.

Nemecek-Marshall, M., MacDonald, R. C., Franzen, J. J., Wojciechowski, C. L. and Fall, R.: Methanol Emission from Leaves (Enzymatic Detection of Gas-Phase Methanol and Relation of Methanol Fluxes to Stomatal Conductance and Leaf Development), Plant Physiol., 108(4), 1359–1368, doi:10.1104/pp.108.4.1359, 1995.

Niinemets, Ü.: What Are Plant-Released Biogenic Volatiles and How They Participate in Landscape- to Global-Level Processes?, in Perera A., Peterson U., Pastur G., Iverson L. (eds) Ecosystem Services from Forest Landscapes, pp. 29–56, Springer, Cham., https://doi.org/10.1007/978-3-319-74515-2_3., 2018.

Niinemets, Ü., Kännaste, A. and Copolovici, L.: Quantitative patterns between plant volatile emissions induced by biotic stresses and the degree of damage, Front. Plant Sci., 4:262, 1–15, doi:10.3389/fpls.2013.00262, 2013.

Noe, S. M., Hüve, K., Niinemets, Ü. and Copolovici, L.: Seasonal variation in vertical volatile compounds air concentrations within a remote hemiboreal mixed forest, Atmos. Chem. Phys., 12(9), 3909–3926, doi:10.5194/acp-12-3909-2012, 2012.

https://doi.org/10.5194/acp-2021-8
Preprint. Discussion started: 29 January 2021


Atmospheric Chemistry and Physics Discussions

Noe, S. M., Niinemets, Ü., Krasnova, A., Krasnov, D., Motallebi, A., Kängsepp, V., Jõgiste, K., Hõrrak, U., Komsaare, K., Mirme, S., Vana, M., Tammet, H., Bäck, J., Vesala, T., Kulmala, M., Petäjä, T. and Kangur, A.: SMEAR Estonia: Perspectives of a large-scale forest ecosystem – atmosphere research infrastructure, Forestry Studies, 63(1), 56–84, doi:10.1515/fsmu-2015-0009, 2015.

Peñuelas, J. and Staudt, M.: BVOCs and global change, Trends Plant Sci., 15(3), 133–144, doi:10.1016/j.tplants.2009.12.005, 2010.

Pöschl, U.: Atmospheric Aerosols: Composition, Transformation, Climate and Health Effects, Angew. Chem., Int. Ed. Engl., 44(46), 7520–7540, doi:10.1002/anie.200501122, 2005.

Praplan, A. P., Tykkä, T., Chen, D., Boy, M., Taipale, D., Vakkari, V., Zhou, P., Petäjä, T. and Hellén, H.: Long-term total OH reactivity measurements in a boreal forest, Atmos. Chem. Phys., 19(23), 14431–14453, doi:10.5194/acp-19-14431-2019, 2019.

Puurunen, J., Tiira, K., Lehtonen, M., Hanhineva, K. and Lohi, H.: Non-targeted metabolite profiling reveals changes in oxidative stress, tryptophan and lipid metabolisms in fearful dogs, Behav. Brain Funct., 12(1), 7, doi:10.1186/s12993-016-0091-2, 2016.

Riipinen, I., Yli-Juuti, T., Pierce, J. R., Petäjä, T., Worsnop, D. R., Kulmala, M. and Donahue, N. M.: The contribution of organics to atmospheric nanoparticle growth, Nature Geosci., 5(7), 453–458, doi:10.1038/NGEO1499, 2012.

Riva, M., Budisulistiorini, S. H., Chen, Y., Zhang, Z., D'Ambro, E. L., Zhang, X., Gold, A., Turpin, B. J., Thornton, J. A., Canagaratna, M. R. and Surratt, J. D.: Chemical Characterization of Secondary Organic Aerosol from Oxidation of Isoprene Hydroxyhydroperoxides, Environ. Sci. Technol., 50(18), 9889–9899, doi:10.1021/acs.est.6b02511, 2016.

Schervish, M. and Donahue, N. M.: Peroxy radical chemistry and the volatility basis set, Atmos. Chem. Phys., 20(2), 1183–1199, doi:10.5194/acp-20-1183-2020, 2020.

Schobesberger, S., D'Ambro, E. L., Lopez-Hilfiker, F. D., Mohr, C. and Thornton, J. A.: A model framework to retrieve thermodynamic and kinetic properties of organic aerosol from composition-resolved thermal desorption measurements, Atmos. Chem. Phys., 18(20), 14757–14785, doi:10.5194/acp-18-14757-2018, 2018.

Ylisirniö, A., Buchholz, A., Mohr, C., Li, Z., Barreira, L., Lambe, A., Faiola, C., Kari, E., Yli-Juuti, T., Nizkorodov, S. A., Worsnop, D. R., Virtanen, A. and Schobesberger, S.: Composition and volatility of secondary organic aerosol (SOA) formed from oxidation of real tree emissions compared to simplified volatile organic compound (VOC) systems, Atmos. Chem. Phys., 20(9), 5629–5644, doi:10.5194/acp-20-5629-2020, 2020a.

Ylisirniö, A., Barreira, L., Pullinen, I., Buchholz, A., Jayne, J., Krechmer, J. E., Worsnop, D. R., Virtanen, A. and Schobesberger, S.: On the calibration of FIGAERO-ToF-CIMS: importance and impact of calibrant delivery for the particle phase calibration, Atmos. Chem. Phys. Discuss., 1–24, doi:10.5194/amt-2020-254, 2020b.

Zhang, H., Yee, L. D., Lee, B. H., Curtis, M. P., Worton, D. R., Isaacman-VanWertz, G., Offenberg, J. H., Lewandowski, M., Kleindienst, T. E., Beaver, M. R., Holder, A. L., Lonneman, W. A., Docherty, K. S., Jaoui, M., Pye, H. O. T., Hu, W., Day, D. A., Campuzano-Jost, P., Jimenez, J. L., Guo, H., Weber, R. J., Gouw, J. de, Koss, A. R., Edgerton, E. S., Brune, W., Mohr, C., Lopez-Hilfiker, F. D., Lutz, A., Kreisberg, N. M., Spielman, S. R., Hering, S. V., Wilson, K. R., Thornton, J. A. and Goldstein, A. H.: Monoterpenes are the largest source of summertime organic aerosol in the southeastern United States, PNAS, 115(9), 2038–2043, doi:10.1073/pnas.1717513115, 2018.

https://doi.org/10.5194/acp-2021-8
Preprint. Discussion started: 29 January 2021

Atmospheric Chemistry and Physics Discussions

700 **Table 1: Groups of oxidation products defined for this study, based on elemental compositions, and their mean, median and maximum concentrations over the campaign period for gas phase (GP) and particle phase (PP) measurements.**

Group of oxidation products	Elemental composition	Mean ($\mu g\ m^{-3}$)		Median ($\mu g\ m^{-3}$)		Max ($\mu g\ m^{-3}$)	
		GP	PP	GP	PP	GP	PP
o-MT	$C_{7\text{-}10}H_{<=(1.8xC)}O_z$	1.4 ± 1.3	0.4 ± 0.4	1.0 ± 0.8	0.3 ± 0.2	6.1	3.1
o-SQT	$C_{13\text{-}15}H_{<=(1.75xC)}O_z$	0.07 ± 0.07	0.1 ± 0.2	0.04 ± 0.03	0.04 ± 0.03	0.4	1.6
Dimers	$C_{>=17}H_{<=(1.8xC)}O_z$	0.003 ± 0.004	0.02 ± 0.03	0.002 ± 0.001	0.01 ± 0.005	0.03	0.2
o-$C_{4\text{-}5}$	$C_{4\text{-}5}H_{<=(2.4xC)}O_z$	3.0 ± 3.1	0.09 ± 0.08	2.0 ± 1.3	0.07 ± 0.03	17.0	0.5
o-highH1 group	$C_{9\text{-}11}H_{(>1.8xC)}O_z$	0.05 ± 0.27	0.06 ± 0.14	0.02 ± 0.01	0.03 ± 0.02	6.1	1.6
o-highH2 group	$C_{>=12}H_{(>1.8xC)}O_z$	0.02 ± 0.03	0.04 ± 0.07	0.01 ± 0.01	0.02 ± 0.01	0.3	0.6
ON	$C_xH_yO_zN_{>0}$	2.6 ± 2.4	0.2 ± 0.2	1.9 ± 1.2	0.2 ± 0.1	16.1	1.0

https://doi.org/10.5194/acp-2021-8
Preprint. Discussion started: 29 January 2021

Atmospheric Chemistry and Physics Discussions

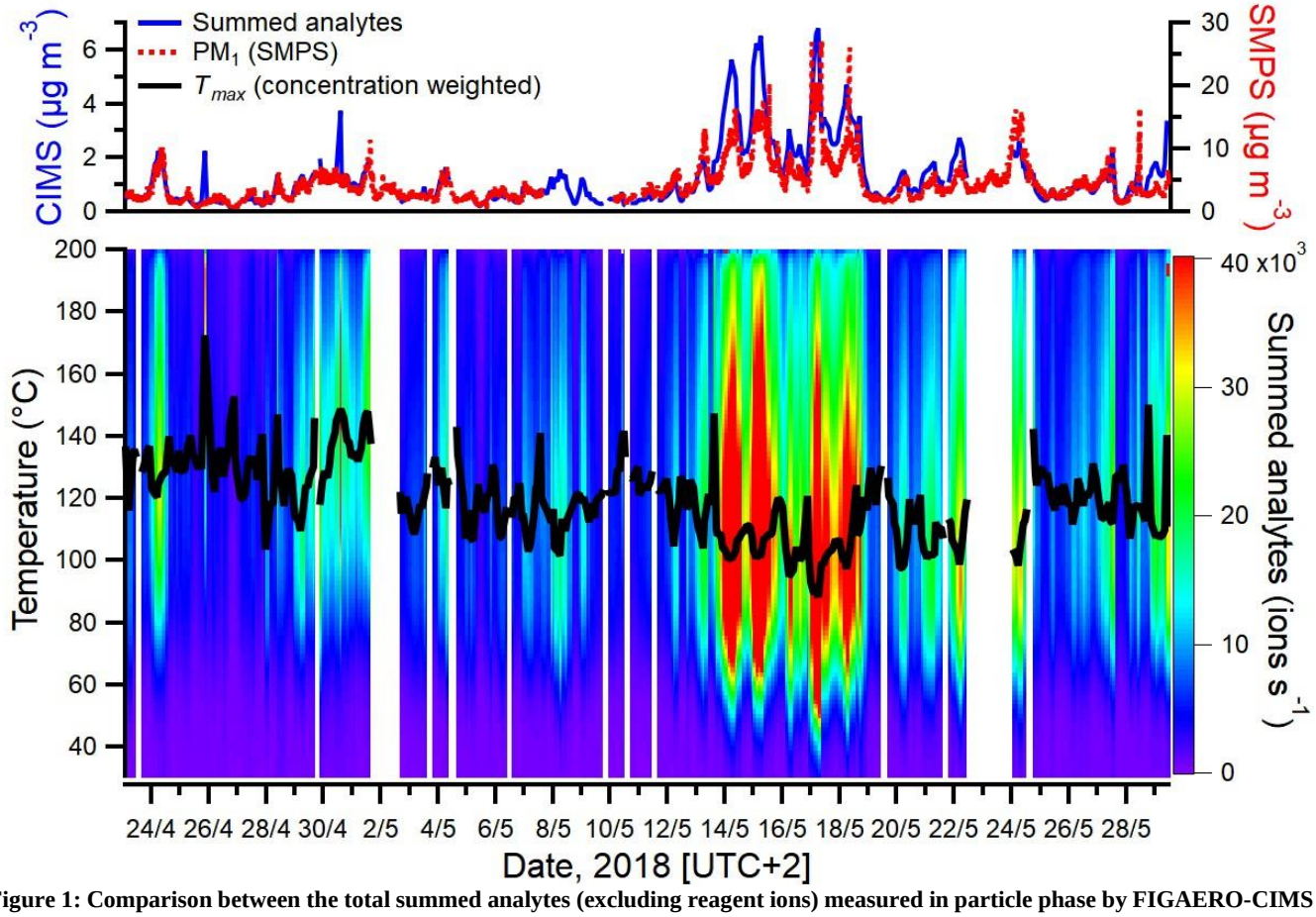

Figure 1: Comparison between the total summed analytes (excluding reagent ions) measured in particle phase by FIGAERO-CIMS and particle mass concentration (PM_1) measured by SMPS (upper panel), and thermograms of the summed analytes during each FIGAERO cycle (lower panel). Black line represents the concentration-weighted T_{max} for each measurement cycle.

https://doi.org/10.5194/acp-2021-8
Preprint. Discussion started: 29 January 2021

Atmospheric Chemistry and Physics Discussions

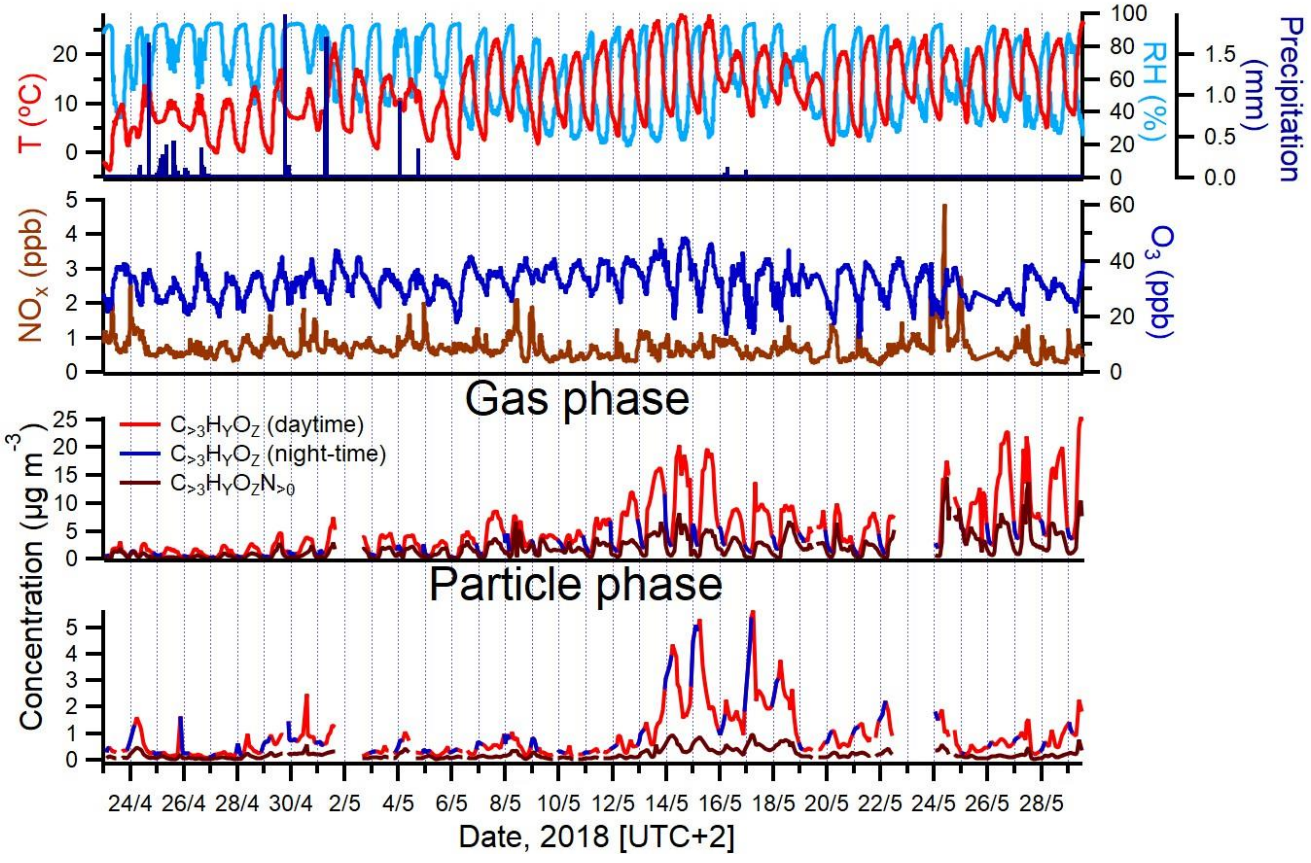

Figure 2: Campaign-spanning comparison between concentrations of larger oxygenated organics measured in the gas and particle phase by FIGAERO-CIMS and colored by time periods of the day (daytime = red, vs. night-time = blue). The evolution of air temperature, RH, precipitation, ozone (O_3) and nitrogen oxides (NO_x = NO + NO_2) is shown as well.

https://doi.org/10.5194/acp-2021-8
Preprint. Discussion started: 29 January 2021

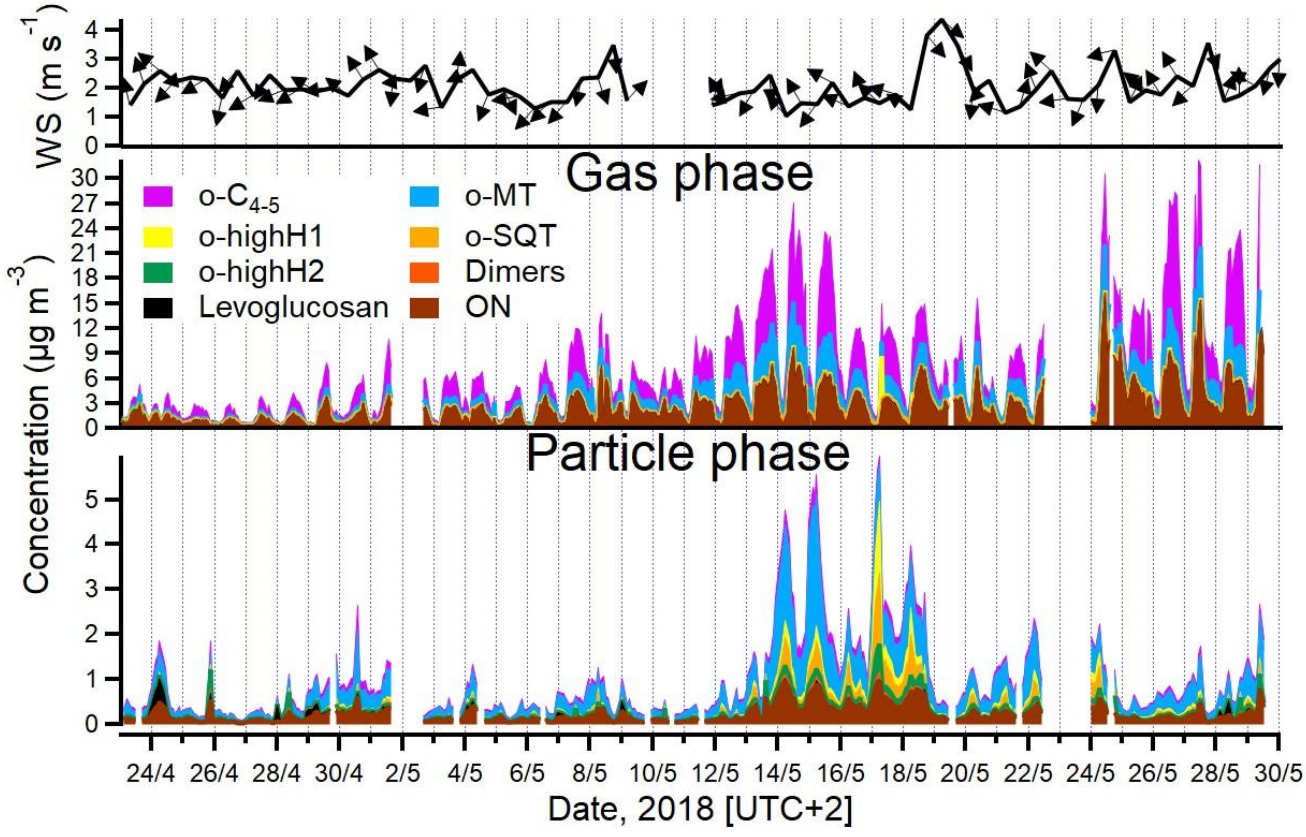

Figure 3: Total mass concentrations of different groups of analytes measured in the gas and particle phase (middle and lower panels), and wind speed and wind direction (upper panel, 12 hours averaged). The group of other measured compounds is excluded for clarity (note that o-highH1 and/or o-highH2 could be misidentified o-SQT/dimers; see text for details).

https://doi.org/10.5194/acp-2021-8
Preprint. Discussion started: 29 January 2021

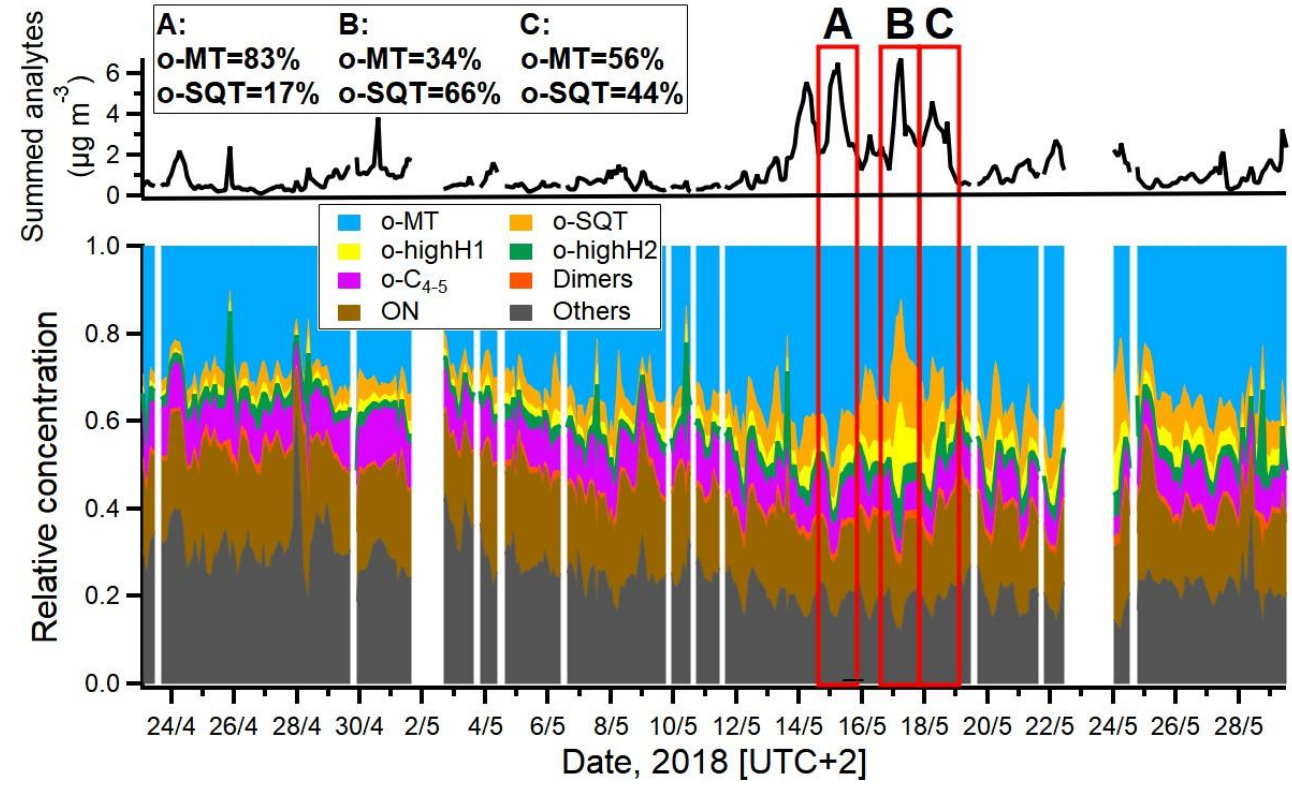

Figure 4: Relative contribution of different groups of analytes to particle mass concentration (lower panel) and total summed analytes (excluding reagent ions) measured by FIGAERO-CIMS (upper panel). The red rectangles indicate the time periods of events A-C. The mass percentages of o-MT ($C_{7-10}H_{<=(1.8xC)}O_z$) and o-SQT ($C_{13-15}H_{<=(1.75xC)}O_z$) during events are also included.

720

https://doi.org/10.5194/acp-2021-8
Preprint. Discussion started: 29 January 2021

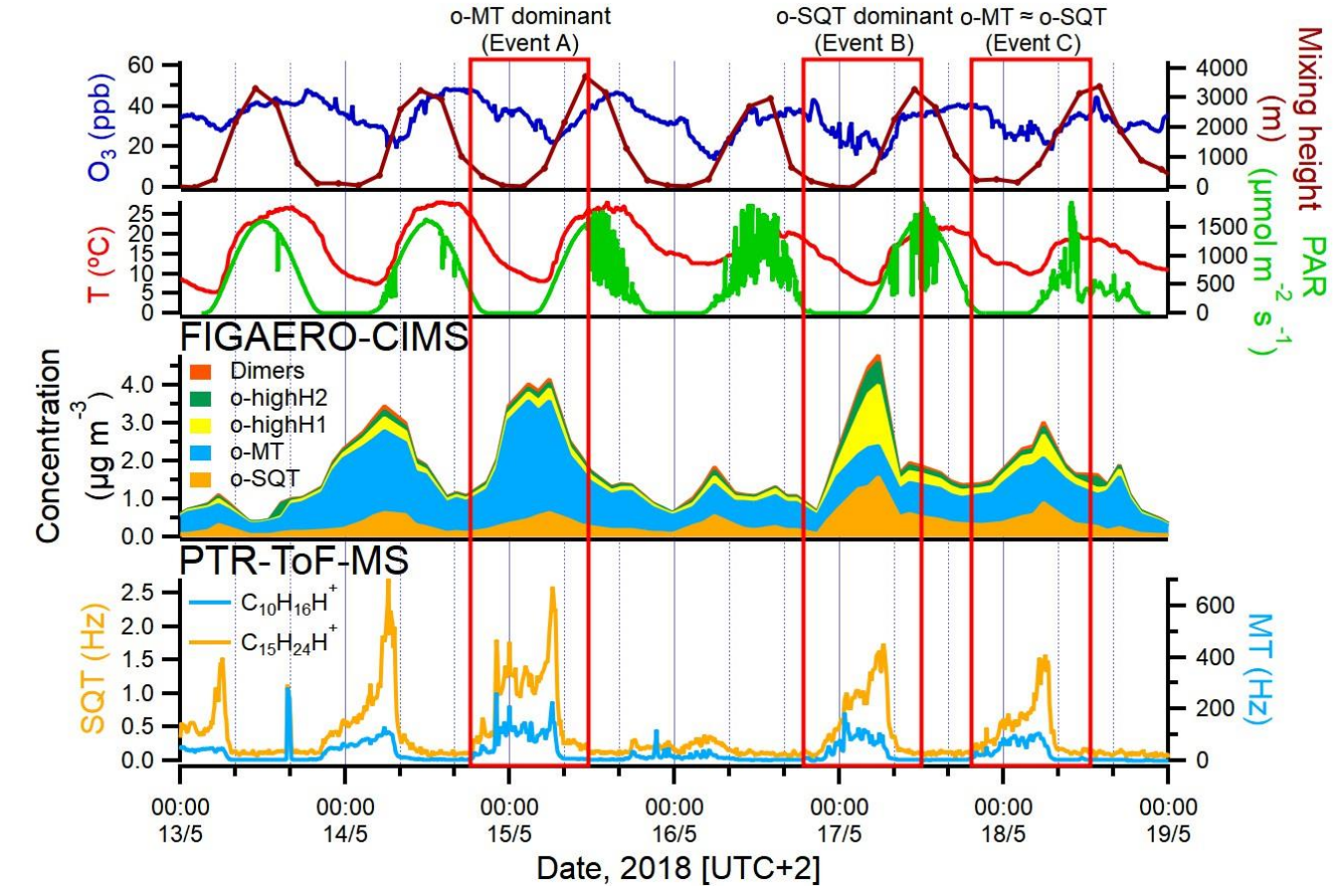

Figure 5: Amounts of monoterpenes and sesquiterpenes measured by PTR-ToF-MS (bottom), concentration of sesquiterpene and monoterpene oxidation products (o-SQT and o-MT) in the particle phase measured by FIGAERO-CIMS (middle), and meteorological parameters (temperature, PAR), mixing height (model-derived), and ozone mixing ratios (top) at the sampling site during the events. The m/z 137 and 205 were used as proxies for monoterpenes and sesquiterpenes, respectively. Note the different axis for sesquiterpenes and monoterpenes.

https://doi.org/10.5194/acp-2021-8
Preprint. Discussion started: 29 January 2021

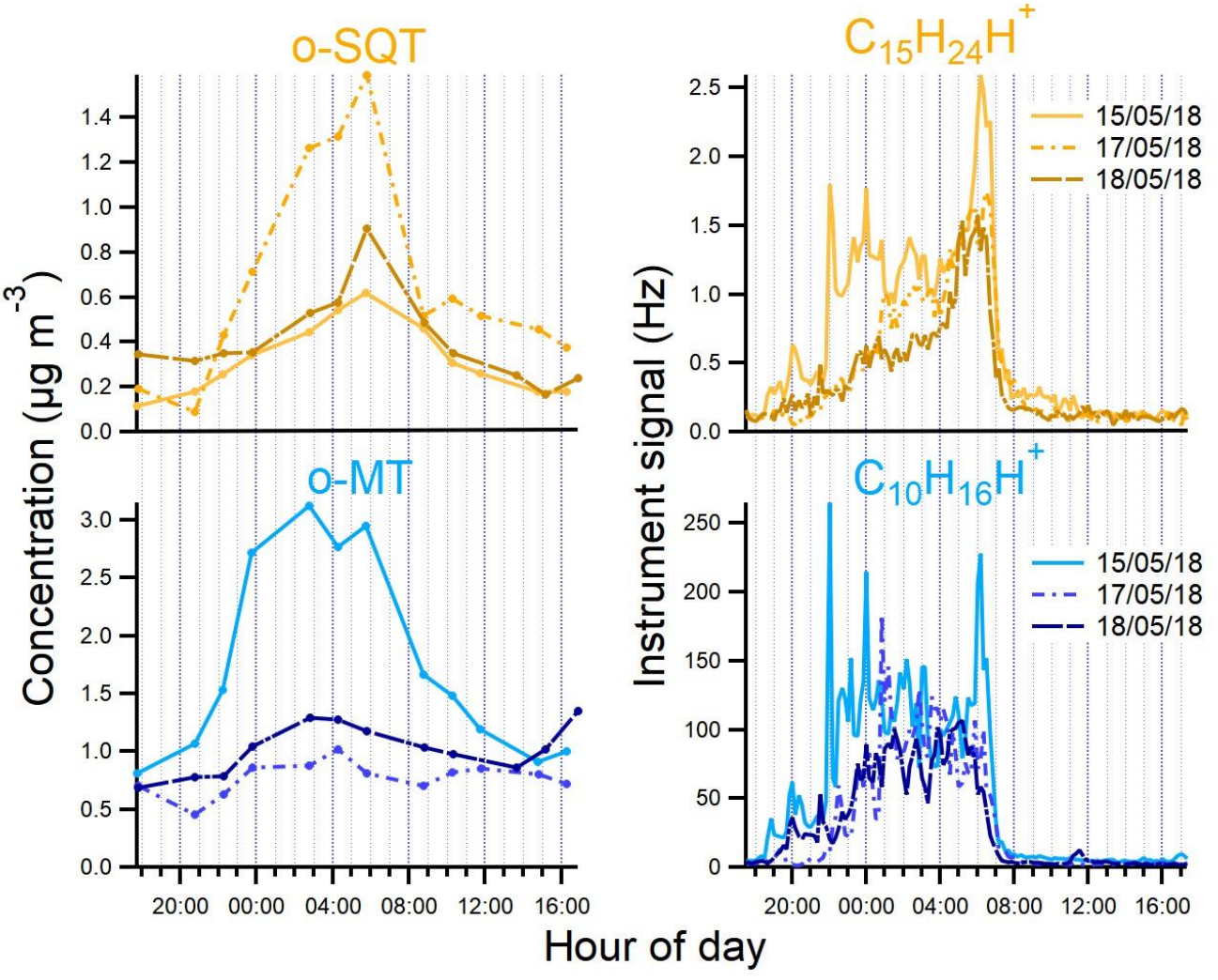

730 **Figure 6: Diurnal variation of o-SQT and o-MT in particle phase measured by FIGAERO-CIMS and of sesquiterpenes and monoterpenes measured by PTR-ToF-MS during the events described in this study.**

https://doi.org/10.5194/acp-2021-8
Preprint. Discussion started: 29 January 2021

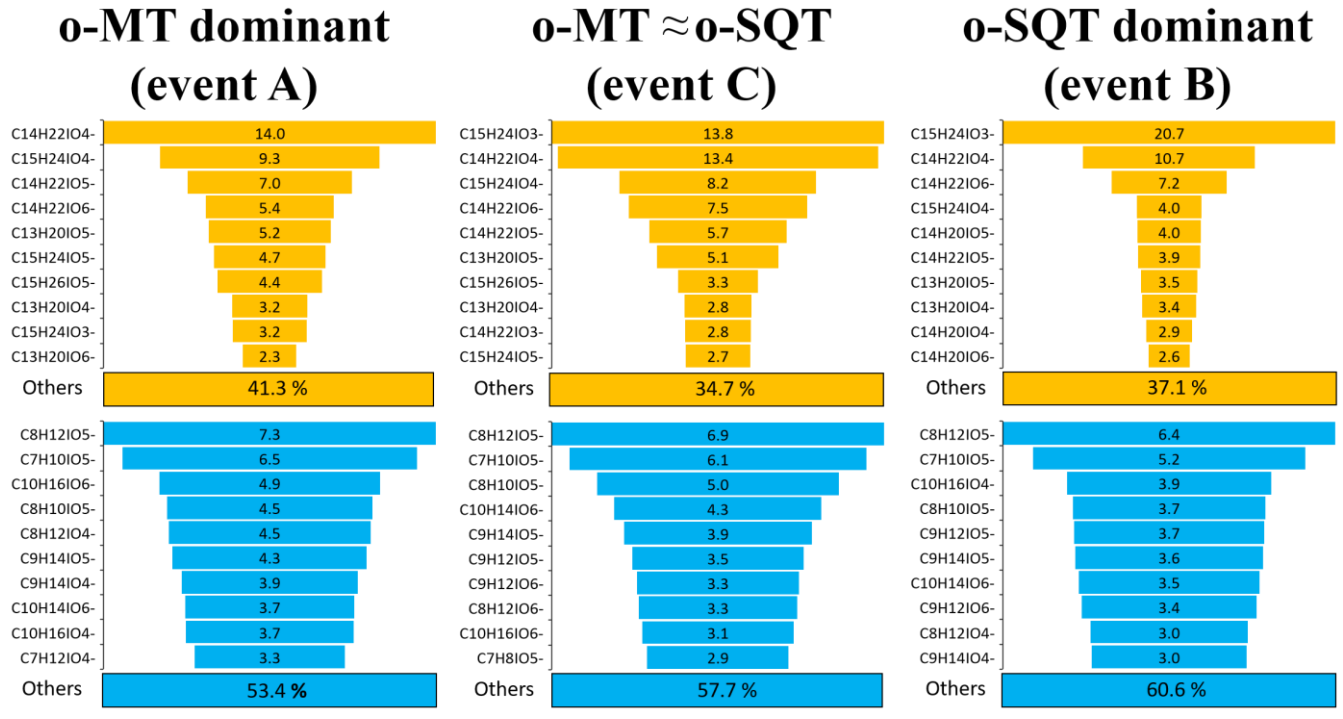

Figure 7: Mass-based contribution of the 10 most abundant chemical formulas to all sesquiterpene (o-SQT, upper row) or monoterpene oxidation products (o-MT, lower row), determined by FIGAERO-CIMS, during the studied events A, B, and C (cf. Fig. 4). Note that the chemical formulas differ between the events. The percentages below each of the six sub-plots indicate the mass-based contribution of the remaining sesquiterpene and monoterpene oxidation products.

https://doi.org/10.5194/acp-2021-8
Preprint. Discussion started: 29 January 2021

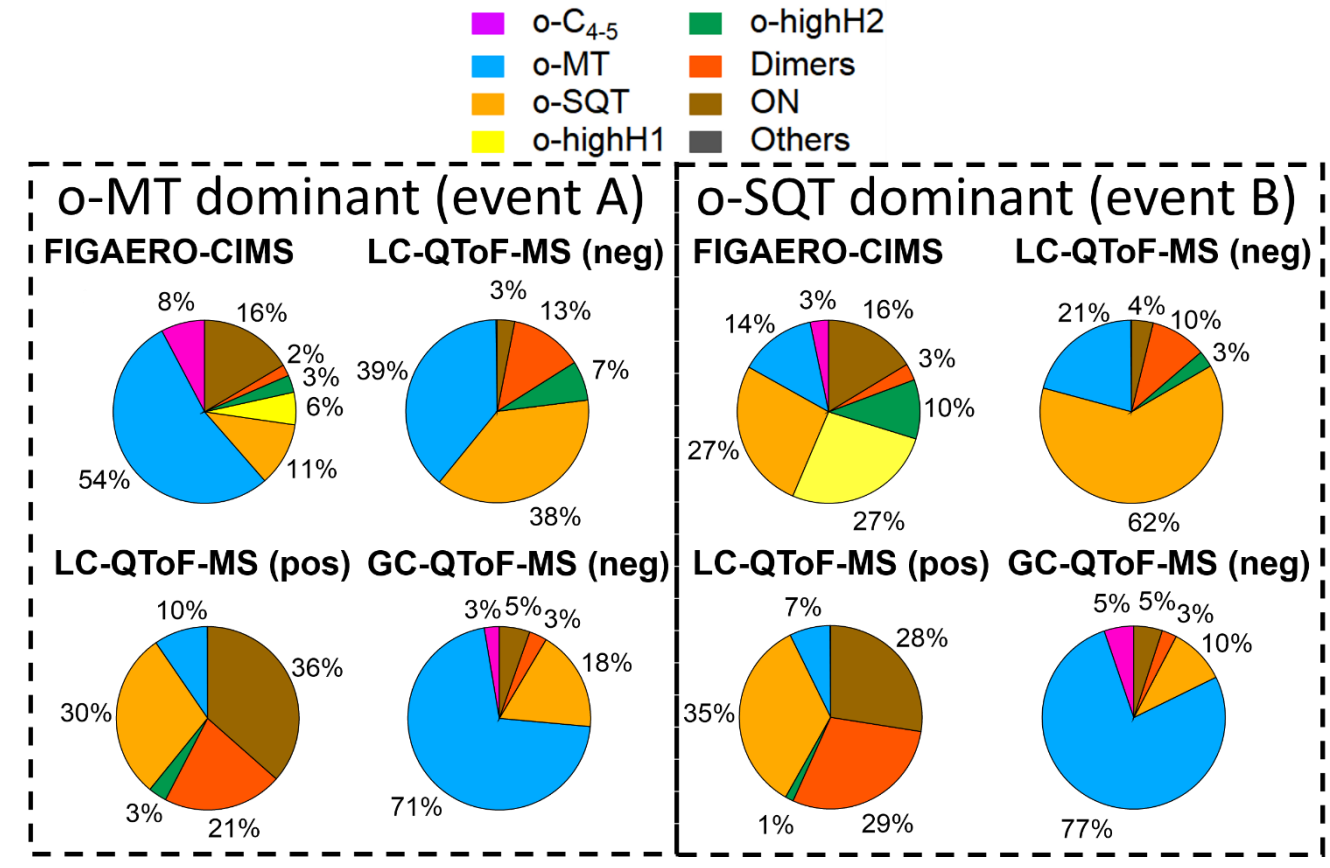

Figure 8: Relative amounts of groups of analytes defined in this study during periods covering event A and event B. The single measurement cycle with maximum concentrations during the corresponding events were selected for FIGAERO-CIMS (15.05.2018 at 05:44:52 for event A and 17.05.2018 at 05:46:40 for event B), while the off-line collection periods between 11.05.2018-15.05.2018 for event A and between 15.05.2018-19.05.2018 for event B were used for LC-QToF-MS and GC-QToF-MS measurements.

https://doi.org/10.5194/acp-2021-8
Preprint. Discussion started: 29 January 2021

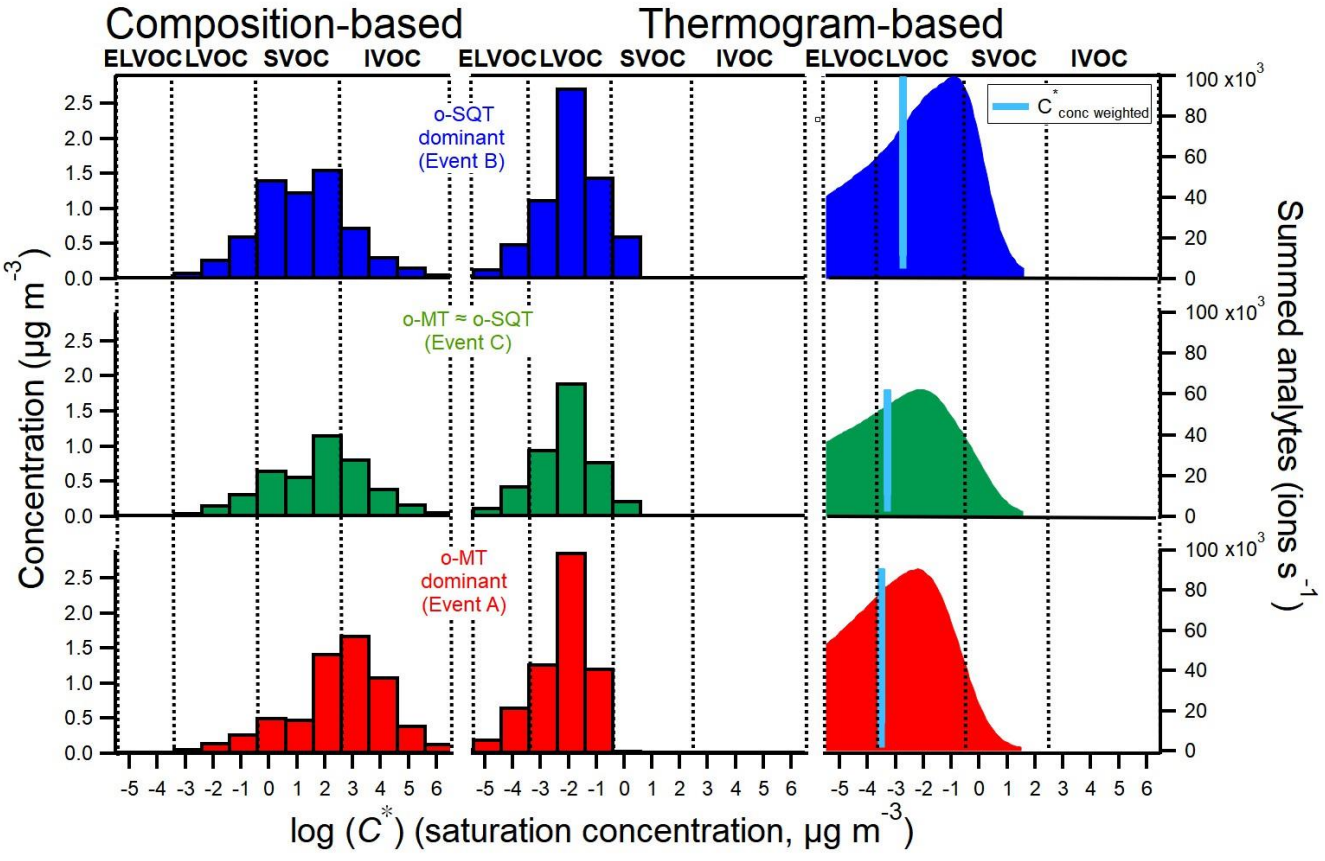

Figure 9: Volatility distribution of analytes measured in particle phase during the three event periods (top: SQT event B; middle: mixed event C; bottom: MT event A), derived using two fundamentally different methods (based on tentatively assigned composition and based on thermograms (T_{max}) as described in Sect. 2.3). The right plots were obtained by converting the desorption temperatures to C^* (Sect. 3.2.4). The blue line indicates the C^* weighted by the summed analytes.

https://doi.org/10.5194/acp-2021-8
Preprint. Discussion started: 29 January 2021

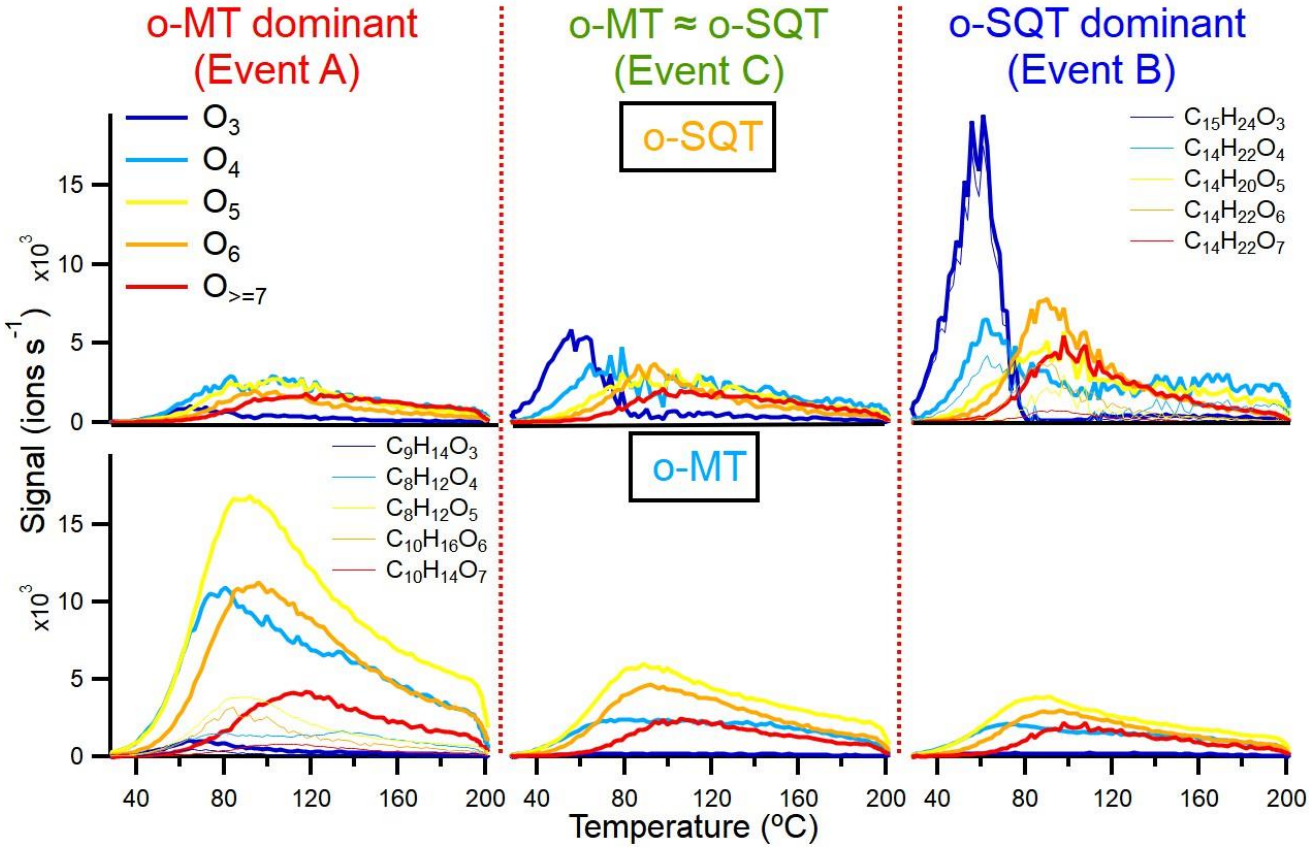

Figure 10: Thermograms obtained from the sum of subsets of o-SQT ($C_{13\text{-}15}H_{<=(1.75xC)}O_z$; top row) and o-MT ($C_{7\text{-}10}H_{y<=(1.8xC)}O_z$; bottom row) analytes during the events investigated in this study (A at the left, C in the center, B at the right). Each subset is the sum over chemical formulas with a certain number of oxygen atoms (indicated by colors). The thin lines represent the five most abundant o-SQT and o-MT for each oxygen-containing subset (for clarity only in the upper right and lower left panel, respectively) during the corresponding event periods.